Magnetization of ferrofluids with dipolar interactions: A Born–Mayer expansion

B. Huke and M. Lücke

Institut für Theoretische Physik,Universität des Saarlandes, D-66041 Saarbrücken, Germany

(February 1, 2008)

Abstract

For ferrofluids that are described by a system of hard spheres interacting via dipolar forces we evaluate the magnetization as a function of the internal magnetic field with a Born–Mayer technique and an expansion in the dipolar coupling strength. Two different approximations are presented for the magnetization considering different contributions to a series expansion in terms of the volume fraction of the particles and the dipolar coupling strength.

PACS: 75.50Mm, 05.70.Ce, 05.20.Jj

I. INTRODUCTION

Ferrofluids [1] are suspensions of ferromagnetic particles of about 10 nm diameter in a carrier fluid. The particles are stabilized against aggregation by coating with polymers or by electrostatic repulsion of charges brought on their surface. On macroscopic scales, ferrofluids can be described as liquids with intrinsic superparamagnetic properties.

In this paper, we are concerned with the equilibrium magnetization M as a function of the internal magnetic field H for given temperature and particle concentration. Sufficiently low concentrated ferrofluids behave like a paramagnetic gas. Therein the interaction between the particles can be neglected and the equilibrium magnetization can be described properly by the Langevin function. The magnetic properties are then necessarily weak. To produce ferrofluids with strong magnetic properties one has to have either a higher particle concentration or one has to use ferromagnetic material with a large bulk magnetization, e. g., cobalt instead of magnetite. In both cases the magnetization is strongly influenced by dipole–dipole and other interactions between the particles.

Several models of dipolar interacting systems have been studied in the literature. Numerical investigations were based on density functional approaches [2–6] and Monte Carlo simulations [7–14]. The models differ in the treatment of the short range interactions, which were described by hard sphere [4,8,9,13–15], other hard core potentials [4,12], soft sphere [7,10], or Lenard–Jones potentials [2,3,6,7,11]. These investigations were mainly undertaken to reveal the phase transition properties. These properties are substantially different for different short range interactions. Thus, for example the question whether a system of particles interacting via long range dipolar forces shows without any dispersive energy, e. g., from attractive van der Waals energy a "liquid–vapor" phase coexistence of a dense and a less dense phase is currently being discussed [7,12,14–18].

Analytical models focus mainly on the equilibrium magnetization in the gas phase (were the term "gas" refers, as far as ferrofluids are addressed, to the magnetic particle subsystem within the liquid carrier). Such models are the Onsager model [19], the Weiss model [20], the

mean spherical approximation [21], and an approach by Buyevich and Ivanov [22] (called high temperature approximation in [23]). These models were tested experimentally for ferrofluids [23–26]. Especially the mean spherical model and the high temperature approximation showed good results [23].

Our approach assumes the magnetic particles in the ferrofluid to be hard spheres with a common diameter D and dipolar moment m. We use the technique of the Born–Mayer expansion [27] together with an expansion in the strength of the dipolar coupling to get analytical approximations. They are obtained via series expansions of the free energy in terms of two parameters: (i) the volume fraction of the hard core particles ϕ and (ii) a dimensionless dipolar coupling constant ϵ, given by the ratio between a typical dipolar energy for particles in hard core contact and the thermal energy kT. Our result for the magnetization goes beyond the high temperature approximation [22] and reduces to it in linear order in ϕ and ϵ.

Dipolar forces fall off as r^{-3} and are thus of long range nature. This long range character requires great care when invoking the thermodynamic limit [28–30]. To circumvent the problem we model the dipolar fields that are generated by distant particles by a magnetic continuum field (similar to the treatment in the Weiss model) while incorporating the near field contributions explicitly in a statistical mechanical description. The magnetization M is then derived as a function of the internal magnetic field H. The so obtained relation $M(H)$ is independent of the probe geometry. Once $M(H)$ is known, the magnetization for a given geometry can in principle be derived by solving the macroscopic Maxwell equations. This may practically still be a difficult task, at least as long as the external field is small or absent. In this case it is known that the magnetization will show for general shaped probes a nontrivial spatial variation at high enough densities [5,6].

Since our method yields an expression for the free energy of the model system we can in principle calculate also other thermodynamic quantities and in particular address the questions of phase transition, e. g., between gas and liquid or between ferromagnetic and non–ferromagnetic phases. We have not addressed the question of a gas–liquid transition of

the magnetic particles suspended in the ferrofluid since it is believed that short range van der Waals–like attractions would have to be incorporated to model real ferrofluids appropriately in this regard [10]. However, the question whether a strong dipolar coupling induces in zero external field a spontaneous magnetization that is currently debated in the literature [2,3,8,9,31,32] is briefly touched upon in Sec. VI A of this paper.

The paper is organized as follows: In Sec. II we discuss the connections between the various fields that are of relevance in a ferrofluid. We present the model to treat the long range dipolar forces. In Sec. III we present the expansion method to get analytical solutions in terms of the two small parameters ϵ and ϕ. In Sec. IV we calculate an expression for the magnetization that contains only linear terms in ϕ but, at least in principle, arbitrary high orders in ϵ. In Sec. V a different expression is derived containing also quadratic terms in ϕ but also only up to second order terms in ϵ. In Sec. VI we discuss our findings and investigate the applicability of the results in the ϕ–ϵ plane. Sec. VII contains a short conclusion.

II. MAGNETIC FIELDS AND MAGNETIZATION

We are interested in the effect of dipolar interactions of the magnetic particles in a ferrofluid on the equilibrium magnetization of the ferrofluid. To that end we consider the ferrofluid as an ensemble of identical spherical particles of diameter D, each carrying a magnetic moment of magnitude m. These particles interact with each other via magnetic dipole–dipole interactions and a hard core repulsion with hard core diameter D. We assume $D \geq D_{mag}$ where D_{mag} is the diameter of the magnetic core of the particles thus allowing for a surfactant surface layer that provides a steric repulsion.

The particles can lower their potential energy by orienting their magnetic moments parallel to a local magnetic field. However any interaction of the particles with the fluid medium they are suspended in is ignored. The latter is taken to be magnetically inert.

A. Different magnetic fields

Before we outline in Sec. II B how we determine in principle the magnetization of the ferrofluid we should like to review briefly the different magnetic fields that one has to distinguish and that are of importance in a system with dipolar interactions. The first field is the external magnetic field $\mathbf{H}_e$ that is applied outside of the probe. If dipolar interactions can be neglected, $\mathbf{H}_e$ is also the field at the position of the particles – at least as long as the carrier fluid can be treated a magnetic vacuum which we will assume throughout the paper. In the presence of dipolar interactions additional fields have to be considered. One of them is the internal field $\mathbf{H}$, that is the macroscopic field inside the probe. By assuming that the equation of state $\mathbf{M}(\mathbf{H})$ is known, $\mathbf{H}$ can be calculated by the common methods of continuum magnetostatics. But the macroscopic field $\mathbf{H}$ differs in general from the field $\mathbf{H}_{local}$ that the magnetic particles feel.

So far one has employed in the ferrofluid literature two models to calculate $\mathbf{H}_{local}$ from $\mathbf{H}$ that are similar in spirit, namely the Weiss model [20] and the Onsager model [19]. Both introduce a virtual hollow sphere inside a magnetic continuum such that the sphere contains a single magnetic particle in its center. The Weiss model assumes the magnetization $\mathbf{M}$ and the internal field $\mathbf{H}$ to be constant everywhere in the magnetic continuum surrounding the sphere. Then the field inside the sphere is given by

$$\mathbf{H}_s = \mathbf{H} + \frac{\mathbf{M}}{3} \quad . \tag{2.1}$$

This is the field that the single magnetic particle feels within the Weiss model, i. e. $\mathbf{H}_{local} = \mathbf{H}_s$.

The Onsager model, on the other hand, is restricted to linearly responding fluids and calculates the field inside the sphere on the assumption that it is really hollow and that therefore $\mathbf{H}$ and $\mathbf{M}$ differ near the sphere from its bulk values. In that case the field within the sphere is

$$\mathbf{H}_{local} = \frac{3\chi + 3}{2\chi + 3}\mathbf{H} \quad . \tag{2.2}$$

χ is the susceptibility. In both models the magnetization is calculated as the magnetization of a system of *noninteracting* dipoles in the magnetic field $\mathbf{H}_{local}$, i. e.,

$$M = M_{sat}\mathcal{L}\left(\frac{m}{kT}H_{local}\right) \quad . \tag{2.3}$$

Here

$$M_{sat} = \frac{N}{V}\frac{m}{\mu_0} \tag{2.4}$$

is the saturation magnetization of the fluid, $\mathcal{L}$ the Langevin function, m the magnetic moment of the particles, and N/V their number density. In the Onsager model the Langevin function is consistently used only in linear order. Letting $M = \chi H$ on the left hand side of (2.3) and using (2.2) allows to calculate χ.

In the Weiss model the selfconsistent solution $M(H)$ is determined using (2.3) and (2.1). The Onsager and Weiss models differ in the treatment of the back reaction of the particle inside the sphere on the magnetic continuum near the sphere's boundary.

B. Decomposition of fields

Since the magnetic continuum is a macroscopic concept one should be careful when using it on the mesoscopic length scales of the interparticle distances and particle diameters. A first–principle statistical mechanical calculation of the magnetization would start with expressing the energy of the system in terms of the statistical variables of the constituents. In this context the local magnetic field $\mathbf{H}_{local}$ that a magnetic moment, say, at position $\mathbf{x}_i$ feels is of importance. It is composed of two different magnetic fields, the external field $\mathbf{H}_e$ and the dipolar contribution $\mathbf{H}_{dipole}$ from the other $N-1$ particles at positions $\mathbf{x}_j$, possessing a magnetic moment $\mathbf{m}_j$. Thus within the first–principles approach one has $\mathbf{H}_{local} = \mathbf{H}_e + \mathbf{H}_{dipole}$, where

$$\mathbf{H}_{dipole}(\mathbf{x_i}) = \sum_j \frac{3\hat{\mathbf{r}}_{ij}(\mathbf{m}_j \cdot \hat{\mathbf{r}}_{ij}) - \mathbf{m}_j}{4\pi\mu_0 r_{ij}^3} \quad . \tag{2.5}$$

Here $\mathbf{r}_{ij} = \mathbf{x_i} - \mathbf{x_j}$, $r_{ij} = |\mathbf{r}_{ij}|$, and $\hat{\mathbf{r}}_{ij} = \mathbf{r}_{ij}/r_{ij}$.

The long range character of the dipolar forces requires special care when invoking the thermodynamic limit $V \to \infty$ and $N \to \infty$ (N/V = const.) — for a critical discussion see, e.g., Ref. [29,28]. The reason is that the dipolar contribution (2.5) will in general depend on the geometry of the ferrofluid probe and the location of $\mathbf{x_i}$ within it. Thus the equilibrium magnetization of a probe in an external field will in general depend on the geometry of the latter and furthermore it will be spatially varying. We therefore use here an approach similar to the one that has been used successfully in solid state theory [33] to determine, e. g., the crystal field splitting caused by local fields. It properly accounts for the contributions from microscopic and macroscopic scales.

Consider some magnetic particle i in a ferrofluid probe in thermodynamic equilibrium. The particles beyond some distance R_s from $\mathbf{x}_i$ can be considered as independent from particle i if R_s is larger than the correlation length induced by the dipolar interactions. Furthermore, if R_s is large enough, their contribution to the local field at $\mathbf{x}_i$ can be approximated by a contribution from a magnetic continuum with equilibrium magnetization $\mathbf{M}$ and macroscopic field $\mathbf{H}$. We assume that the distance R_s is still small compared to the length scale on which the macroscopic fields $\mathbf{M}$ and $\mathbf{H}$ vary. Thus we introduce a virtual sphere of radius R_s around particle i (dark particle in the center of Fig. 1) to separate the dipolar field into a "far" and a "near" contribution

$$\mathbf{H}_{dipole,far}(\mathbf{x}_i) = \sum_{r_{ij}>R_s} \frac{3\hat{\mathbf{r}}_{ij}(\mathbf{m}_j \cdot \hat{\mathbf{r}}_{ij}) - \mathbf{m}_j}{4\pi\mu_0 r_{ij}^3} \quad , \tag{2.6}$$

$$\mathbf{H}_{dipole,near}(\mathbf{x}_i) = \sum_{r_{ij}<R_s} \frac{3\hat{\mathbf{r}}_{ij}(\mathbf{m}_j \cdot \hat{\mathbf{r}}_{ij}) - \mathbf{m}_j}{4\pi\mu_0 r_{ij}^3} \quad . \tag{2.7}$$

Then

$$\mathbf{H}_{local} = \mathbf{H}_e + \mathbf{H}_{dipole,far} + \mathbf{H}_{dipole,near} \quad . \tag{2.8}$$

If the sphere would be empty, $\mathbf{H}_e + \mathbf{H}_{dipole,far} = \mathbf{H}_s$ would be the local field inside the sphere.

A key point of our treatment is to express the far field $\mathbf{H}_{dipole,far}$ within the continuum approximation. Using this approach the field in the empty sphere is given by $\mathbf{H}_s = \mathbf{H} + \mathbf{M}/3$

(2.1). Note that this approximation is not valid near the sphere's boundary. But at the center of the sphere $\mathbf{H}_{local}$ consists of the continuum contribution $\mathbf{H}_s$ from the far region and the contribution for the dipoles within the sphere:

$$\mathbf{H}_{local} = \mathbf{H}_s + \mathbf{H}_{dipole,near} = \mathbf{H} + \frac{\mathbf{M}}{3} + \mathbf{H}_{dipole,near} \quad . \tag{2.9}$$

This result agrees with Eq. (27.26) of Ref. [33] where it has been derived with slightly different arguments for electric dipoles. Due to the long range character of the dipolar forces $\mathbf{H}_{dipole}$ will be in general geometry dependent and spatially varying. $\mathbf{H}_s$, respectively $\mathbf{H}$ and $\mathbf{M}$ will then also show these features as mentioned above.

If the dipolar coupling between the particles is so weak that even the dipolar fields of the nearest neighbours of particle i can be described by a continuum field, i. e., if R_s can be chosen as being smaller than the mean distance between the particles, we can drop the contribution $\mathbf{H}_{dipole,near}$ altogether and arrive at the Weiss model, where a single particle is located inside the hollow sphere in the continuum.

C. Equilibrium magnetization

We want to determine the thermodynamic equilibrium relation $M(H)$ between the magnetization

$$\mathbf{M} = \frac{1}{\mu_0 V} \sum_i \langle \mathbf{m}_i \rangle = \frac{N}{\mu_0 V} \langle \mathbf{m} \rangle \tag{2.10}$$

and the macroscopic magnetic field $\mathbf{H}$ in the thermodynamic limit. Instead of considering the dipolar interaction of all particles in an external field in the statistical mechanical problem (2.10) we take explicitly only interactions between those particles into account whose distance is smaller than the sphere radius R_s. The other interactions are represented by the far–field continuum approximation $\mathbf{H}_s = \mathbf{H} + \mathbf{M}/3$. The magnetization $M_{sphere}(H_s)$ resulting from this decomposition of fields is then identified with the equilibrium magnetization $M(H)$ of the ferrofluid

$$M_{sphere}(H + M/3) = M(H) \ . \tag{2.11}$$

Thus after having obtained the approximate expressing for M_{sphere} as a function of $H + M/3$ we then obtain from solving (2.11) for M an approximation for the sought after equilibrium relation $M(H)$. The functional dependence of M on H is independent of the probe geometry.

In the limit of weak dipolar coupling or when R_s becomes smaller than the mean distance between the particles we find $M_{sphere} = M_{sat}\mathcal{L}\left[\frac{m}{kT}(H + M/3)\right]$ so that the Weiss model is recovered as discussed above.

The magnetization M_{sphere} in (2.11) depends on two dimensionless parameters that characterize the thermodynamic state of the ferrofluid. One of these parameters is the volume concentration of the particles

$$\phi = \frac{N}{V}\frac{\pi D^3}{6} \ . \tag{2.12}$$

The ratio ϕ_{mag} of the volume of the magnetic material to the total volume is $\phi_{mag} = (D_{mag}/D)^3\phi$. The other parameter is

$$\epsilon = \frac{m^2}{4\pi\mu_0 kTD^3} \ , \tag{2.13}$$

the ratio between a typical energy of dipole–dipole interaction of particles in contact (i. e., at the distance of the hard core diameter D) and the thermal energy kT.

III. CANONICAL PARTITION FUNCTION

We use the canonical ensemble average to evaluate M_{sphere}. Given a system of N interacting particles with an interaction potential V_{ij} $(1 < i, j < N)$ and external potential per particle V_i, the canonical partition function is given by

$$Z = \int e^{-\sum_k v_k - \sum_{i<j} v_{ij}} \, d\Gamma \ . \tag{3.1}$$

Here $v_i = V_i/kT$, $v_{ij} = V_{ij}/kT$, and $d\Gamma$ means integration over the configuration space. In our case, a configuration is characterized by specifying the position vector $\mathbf{x}_i$ and two angles

for each magnetic particle. The two angles define the direction of the magnetic moment $\mathbf{m}_i$. The modulus m is assumed to be constant and the same for all particles. Note that we ignore any translational and rotational degrees of freedom of the particles that carry the magnetic moments, since they have no effect on the magnetization. Only the locations of the moments, i. e., of the particles and the orientations of the moments are considered as statistical variables.

In the first–principles statistical mechanical problem identified by a superscript 0, the external potential would be the energy of a dipole in the external magnetic field

$$V_i^0 = -\mathbf{m}_i \cdot \mathbf{H}_e \quad . \tag{3.2}$$

The interparticle potential is modelled by a dipole–dipole (DD) interaction plus hard core (HC) repulsion. Thus

$$V_{ij}^0 = V_{ij}^{0,DD} + V_{ij}^{HC} \quad , \tag{3.3}$$

$$V_{ij}^{0,DD} = -\frac{3(\mathbf{m}_i \cdot \hat{\mathbf{r}}_{ij})(\mathbf{m}_j \cdot \hat{\mathbf{r}}_{ij}) - \mathbf{m}_i \cdot \mathbf{m}_j}{4\pi\mu_0 r_{ij}^3} \quad , \tag{3.4}$$

$$V_{ij}^{HC} = \begin{cases} 0 & \text{for } r_{ij} > D \\ \infty & \text{for } r_{ij} < D \end{cases} \quad . \tag{3.5}$$

The replacement of the dipolar magnetic fields from far–away particles by a field that has its origin in a magnetic continuum results in a new canonical partition function with the "external" potential of a dipole

$$V_i = -\mathbf{m}_i \cdot \mathbf{H}_s \quad , \tag{3.6}$$

in the field $\mathbf{H}_s = \mathbf{H} + \mathbf{M}/3$ and a dipolar interaction term with a cutoff, i. e.,

$$V_{ij}^{DD} = \begin{cases} V_{ij}^{0,DD} & \text{for } r_{ij} < R_s \\ 0 & \text{for } r_{ij} > R_s \end{cases} \quad . \tag{3.7}$$

Note that when using (3.6) and (3.7) in the expression (3.1) for the partition function we describe every particle i as being at the center of a sphere of radius R_s inside a magnetic continuum such that each particle feels the "external" field $\mathbf{H}_s$ and explicit dipolar fields $\mathbf{H}_{dipole,near}(\mathbf{x}_i)$ (2.7) from the particles whose distance is smaller than R_s.

The aforementioned statistical mechanical problems with the long range nature of the bare dipolar interactions is thus circumvented by the cutoff at R_s in (3.7) that results from decomposing dipolar fields into a near and a far contribution. Dipolar forces appear explicitly only as forces with a finite range. Their influence on the magnetization in our approach is therefore independent of the geometry of the probe. The geometry dependence enters only via the effective "external" field H_s from the far field contribution.

A. Born–Mayer expansion method

Since an integral such as (3.1) is hard to solve even numerically we use the Born–Mayer expansion method [27] to get analytical results. The key point of this method is to write

$$Z = \int \prod_k e^{-v_k} \prod_{i<j} (1 + f_{ij})\, d\Gamma \quad , \tag{3.8}$$

where

$$f_{ij} = e^{-v_{ij}} - 1 \quad . \tag{3.9}$$

If the typical interaction energy is small compared to kT, the f_{ij} can be considered as small parameters, and Z can be expanded into a series:

$$\begin{aligned} Z = & \int \prod_m e^{-v_m}\, d\Gamma + \\ & \int \prod_m e^{-v_m} \sum_{i<j} f_{ij}\, d\Gamma + \\ & \int \prod_m e^{-v_m} \sum_{i<j} f_{ij} \sum_{k<l} f_{kl}\, d\Gamma + \\ & \ldots \quad . \end{aligned} \tag{3.10}$$

These integrals can be factorized and are therefore easier to handle.

The first order of (3.10) contains terms like

$$\int \prod_m e^{-v_m} e^{-v_{12}^{DD} - v_{12}^{HC}} \; d\,\vec{\mathbf{x}}\; d\,\vec{\Omega} \quad . \tag{3.11}$$

Here $d\,\vec{\mathbf{x}}\; d\,\vec{\Omega}$ is an abbreviation for $d\mathbf{x}_1 ... d\mathbf{x}_N d\Omega_1 .. d\Omega_N$, and $d\Omega_i$ means the integration over the possible orientations of $\mathbf{m}_i$.

B. Expansion in powers of v^{DD}

Obviously even the first order still cannot be evaluated analytically. Therefore a second series expansion is made

$$f_{ij} = e^{-v_{ij}^{HC}} e^{-v_{ij}^{DD}} - 1 = f_{ij}^{(0)} + f_{ij}^{(1)} + f_{ij}^{(2)} + ..., \tag{3.12a}$$

$$f_{ij}^{(0)} = \left(e^{-v_{ij}^{HC}} - 1 \right) \tag{3.12b}$$

$$f_{ij}^{(\alpha)} = \frac{\left(-v_{ij}^{DD} \right)^{\alpha}}{\alpha!} e^{-v_{ij}^{HC}} ... \;\; , \alpha \geq 1 \quad . \tag{3.12c}$$

So we expand f_{ij} in powers of the reduced dipolar interaction v_{ij}^{DD}. The integrals in (3.10) that remain to be solved are of the form

$$\int \prod_m e^{-v_m} f_{ij}^{(\alpha)} f_{kl}^{(\beta)} ... \; d\,\vec{\mathbf{x}}\; d\,\vec{\Omega} \quad . \tag{3.13}$$

We now introduce a modification of the common graphical representation of Born–Mayer integrals as follows

1. Every distinct particle that appears via interaction terms of the form $f_{ij}^{(\alpha)}$ is represented by a circle.

2. A zeroth order interaction term $f_{ij}^{(0)}$ is represented by an overlap of the circles i and j.

3. First, second, ... order interaction is represented by one, two, ... lines connecting the circles.

Note that the representation of the zeroth order dipolar interaction by two overlapping circles is a reminder that in this case the integrand is nonzero only if the particles are assumed to be in a configuration in which they would indeed overlap.

It turns out, that the expansion in terms of the $f_{ij}^{(\alpha)}$ means an expansion in powers of the two parameters ϵ and ϕ, that define the thermodynamical system. Every line in a representing graph, i. e., every power of v_{ij}^{DD} results in a factor ϵ. Every n–particle subgraph in which all circles are connected to each other directly or indirectly gives a factor of ϕ^{n-1}. In the next two sections we will present two expansions considering different terms.

IV. EXPANSION UP TO FIRST ORDER IN ϕ

In this section only terms up to $O(\phi)$ will be taken into account.

A. Partition function

In $O(\phi)$ the canonical partition function reads

$$Z = \int \prod_k e^{-v_k} \, d\,\vec{\mathbf{x}} \, d\,\vec{\Omega} + \int \prod_k e^{-v_k} \sum_{i<j} f_{ij} \, d\,\vec{\mathbf{x}} \, d\,\vec{\Omega} + O(\phi^2) \ . \tag{4.1}$$

The f_{ij} have yet to be expanded in powers of v_{ij}^{DD}. Figure 2 shows the corresponding graphs. There are $N(N-1)/2 \approx N^2/2$ ways to choose i and j. Because all particles are identical one can write

$$Z = \int \prod_k e^{-v_k} \, d\,\vec{\mathbf{x}} \, d\,\vec{\Omega} + \frac{N^2}{2} \int \prod_k e^{-v_k} f_{12} \, d\,\vec{\mathbf{x}} \, d\,\vec{\Omega} + O(\phi^2) \ . \tag{4.2}$$

Integrating over most degrees of freedom results in

$$Z = Z_0 + \frac{N^2}{2} z_0^{N-2} \int e^{-v_1 - v_2} f_{12} \, d\mathbf{x}_1 d\mathbf{x}_2 d\Omega_1 d\Omega_2 + O(\phi^2) \ . \tag{4.3}$$

Here

$$Z_0 = z_0^N \ ; \qquad z_0 = 4\pi V \frac{\sinh \alpha_s}{\alpha_s} \tag{4.4}$$

is the partition function of a paramagnetic gas of noninteracting particles in the field H_s defining the Langevin parameter

$$\alpha_s = \frac{mH_s}{kT} \ . \tag{4.5}$$

B. Expansion in the dipolar interaction

Now we expand f_{12} appearing in (4.3) in a power series in ϵ. The n–th summand of this series contains integrals of the form

$$A_n = \int e^{-v_1 - v_2} f_{12}^{(n)} \, d\mathbf{x}_1 d\mathbf{x}_2 d\Omega_1 d\Omega_2 \ . \tag{4.6}$$

A_0 is special. Here one gets

$$\begin{aligned} A_0 &= \left(4\pi \frac{\sinh \alpha_s}{\alpha_s}\right)^2 \int \left(e^{-v_{12}^{HC}} - 1\right) \, d\mathbf{x}_1 d\mathbf{x}_2 \\ &= \frac{1}{V} z_0^2 \int \left(e^{-v_{12}^{HC}} - 1\right) \, d\mathbf{r}_{12} \ . \end{aligned} \tag{4.7}$$

The integrand vanishes if $r_{12} > D$. Otherwise its value is -1. Thus

$$A_0 = -\frac{4}{3}\pi \frac{D^3}{V} z_0^2 \ , \tag{4.8}$$

or by expressing the result in terms of ϕ

$$A_0 = -\frac{8}{N} \phi z_0^2 \ . \tag{4.9}$$

For $n \geq 1$ we have

$$\begin{aligned} A_n = \frac{1}{n!} \int & e^{-v_1 - v_2} \\ & \times \left(-v_{12}^{DD}\right)^n e^{-v_{12}^{HC}} d\mathbf{x}_1 d\mathbf{x}_2 d\Omega_1 d\Omega_2 \ . \end{aligned} \tag{4.10}$$

Switching from $\mathbf{r}_2$ to the relative coordinate $\mathbf{r}_{12}$ and integrating over $\mathbf{r}_1$ gives a factor of V. Then $\mathbf{r}_{12}$ runs over the sphere volume. We introduce spherical coordinates, i. e.,

$$\begin{aligned}
\mathbf{m}_1 &= m(\cos\varphi_1 \sin\vartheta_1, \sin\varphi_1 \sin\vartheta_1, \cos\vartheta_1) \\
\mathbf{m}_2 &= m(\cos\varphi_2 \sin\vartheta_2, \sin\varphi_2 \sin\vartheta_2, \cos\vartheta_2) \\
\mathbf{r}_{12} &= r_{12}(\cos\varphi \sin\vartheta, \sin\varphi \sin\vartheta, \cos\vartheta) \quad .
\end{aligned} \tag{4.11}$$

The direction of the magnetic field defines the z–axis. Then, the integral assumes the form

$$\begin{aligned}
A_n = \frac{V}{n!} \int & e^{\alpha_s \cos\vartheta_1 + \alpha_s \cos\vartheta_2} \\
& \times \left(\frac{m^2}{4\pi\mu_0 kT r_{12}^3} \right)^n P^n(\varphi_1, \vartheta_1, \varphi_2, \vartheta_2, \varphi, \vartheta) \\
& \times e^{-v_{12}^{HC}} r_{12}^2 dr_{12} d\omega_{12} d\Omega_1 d\Omega_2 \quad .
\end{aligned} \tag{4.12}$$

The new spherical angle ω_{12} represents φ and ϑ. The exact form of the function P is not important, but P and therefore P^n is a polynomial in the cos and sin of the six angles. Integration over four of them can be done analytically. Finally this can also be done for ϑ_1 and ϑ_2 by substituting $u_{1,2} = \cos\vartheta_{1,2}$. One gets an expression of the form

$$A_n = \frac{V}{n!} G_n^*(\alpha_s) \int_D^{R_s} \left(\frac{m^2}{4\pi\mu_0 kT r_{12}^3} \right)^n r_{12}^2 dr_{12} \quad . \tag{4.13}$$

Here we have introduced the correct bounds of the last remaining integral explicitly. By setting the lower bound to D we have incorporated the hard core factor. The upper bound is given by the cutoff radius R_s for the near-field dipolar contribution. While the evaluation of G_n^* can be done analytically, it is quite difficult to do this by hand even for $n = 2$. We therefore used the computer algebra system *mathematica* to perform the integrations. See Appendix A for the form of the G_n^*.

For $n \geq 2$ one can safely set $R_s = \infty$ (see below). For $n = 1$ this would result in a logarithmic divergence of the integral. But $G_1^* \equiv 0$ anyway, because the calculation of G_1^* involves an averaging over a dipolar field. So by using ϵ and ϕ one finally has

$$A_n = \frac{2V^2}{N\pi(n-1)n!} G_n^*(\alpha_s) \epsilon^n \phi \qquad n \geq 2 \quad , \tag{4.14}$$

$$A_1 = 0 \ . \tag{4.15}$$

Note that A_1 vanishes only in our spherical configuration with finite R_s. The divergence of A_1 in the general, spatially unrestricted case is just an expression of fact that the dipolar forces are long range. By treating the distant parts of the ferrofluid as a continuum we incorporate any long-range effects and the resulting geometry dependence via the field $H_s = H + M/3$. Into this field enters the relation between the external and the macroscopic internal field.

Two further comments should be made here. A generalization of our calculation for central symmetric interactions other than a hard sphere potential is possible. It requires an analytical or numerical evaluation of integrals of the form $\int r^{2-3n} e^{-v^{SR}} dr$ in (4.13), with $v^{SR} = V^{SR}/kT$ and V^{SR} denoting the r–dependent short range potential in question.

The second thing is that we can now make quantitative statements about how large the virtual sphere has to be chosen. To ensure A_1 to vanish unambigously in (4.13) and to introduce H_s instead of H_e as "external" field R_s has only to be finite. The larger R_s the better is the modeling of large–distance particle correlations entering into A_n for $n > 1$. Taking the limit $R_s \to \infty$ as the final step in the calculation of the A_n is therefore appropriate from this point of view. On the other hand, the requirement of uniformity of the fields $\mathbf{H}$ and $\mathbf{M}$, that allows us to write $H_s = H + M/3$ restricts R_s to values below the scale on which H and M vary. If one would use a finite radius R_s one would get instead of (4.14) for $n \geq 2$

$$A_n = \frac{2V^2}{N\pi(n-1)n!} G_n^*(\alpha_s)\epsilon^n \phi \left[1 - (D/R_s)^{3n-3}\right] \tag{4.16}$$

which allows an error estimate: Consider a system where $\mathbf{M}$ and $\mathbf{H}$ do not vary on the scale of, say, μm. For ferrofluids, $D \approx 10$ nm. Choosing $R_s = 10D$ or $100D$ is then both allowed and implies a difference in A_2 of about 0.1 percent. The result for $R_s = 100D$ is better than for $R_s = 10D$, because in the latter case particles in a distance range between 100 nm and 1 μm are treated in the continuum approximation and not correctly. But the error that is made by treating the ferrofluid as a continuum already beyond $R_s = 10D$ is only about 0.1 percent. We can safely assume that the macroscopic, magnetic properties do not vary on

this scale. Thus 100 nm is an appropriate medium scale on which both requirements hold: The continuum approximation works well beyond this cutoff radius *and* the macroscopic fields **H** and **M** should be constant on this scale. Except for the calculation of A_1, it is then possible to set $R_s = \infty$ in the calculations of the integrals.

Using the results (4.14), (4.15), (4.9), and (4.6) in (4.3), one gets the following expression for Z:

$$Z = Z_0 \left[1 - 4N\phi + N\phi \sum_{n=2}^{\infty} G_n(\alpha_s)\epsilon^n \right] + O(\phi^2) \quad . \tag{4.17}$$

Here we introduced the functions

$$G_n(\alpha_s) = \frac{1}{16\pi^3(n-1)n!} \left(\frac{\alpha_s}{\sinh \alpha_s} \right)^2 G_n^*(\alpha_s) \quad , \tag{4.18}$$

some of which are given in Appendix A.

C. Free energy and magnetization

The next step is to compute the free energy

$$\begin{aligned} \frac{F}{kT} &= -\ln Z = -N \ln z_0 \\ &\quad - \ln \left[1 - 4N\phi + N\phi \sum_{n=2}^{\infty} G_n(\alpha_s)\epsilon^n \right] \\ &\quad + O(\phi^2) \quad . \end{aligned} \tag{4.19}$$

In $O(\phi)$, we can use $\ln(1+x) = 1 + x$ here:

$$\begin{aligned} \frac{F}{kT} &= -N \ln z_0 + 4N\phi - N\phi \sum_{n=2}^{\infty} G_n(\alpha_s)\epsilon^n \\ &\quad + O(\phi^2) \quad . \end{aligned} \tag{4.20}$$

The magnetization turns out to be

$$\begin{aligned} M_{sphere}(\alpha_s) &= -\frac{1}{\mu_0 V} \frac{\partial F}{\partial H_s} = -\frac{m}{\mu_0 V kT} \frac{\partial F}{\partial \alpha_s} \\ &= \frac{Nm}{\mu_0 V} \left[\mathcal{L}(\alpha_s) + \phi \sum_{n=2}^{\infty} G_n'(\alpha_s)\epsilon^n \right] \\ &\quad + O(\phi^2) \quad . \end{aligned} \tag{4.21}$$

The leading term is the Langevin function $\mathcal{L}$ times the saturation magnetization $M_{sat} = \frac{Nm}{\mu_0 V}$ of the fluid.

In order to determine $M(H)$ we identify, according to (2.11), $M_{sphere}(\alpha_s)$ with $M(\alpha)$, i. e.,

$$\frac{M}{M_{sat}} = \mathcal{L}\left(\alpha + \frac{mM}{3kT}\right) + \phi \sum_{n=2}^{\infty} G_n'\left(\alpha + \frac{mM}{3kT}\right)\epsilon^n + O(\phi^2) \quad , \tag{4.22}$$

where α is the usual Langevin parameter,

$$\alpha = \frac{mH}{kT} \quad . \tag{4.23}$$

Instead of trying to find the function $M(\alpha)$ that solves this equation exactly we expand the functions $\mathcal{L}$ and G_n' for small ϕ into a series around $M = 0$ and reinsert it on the right hand side. Using the fact that $\frac{mM_{sat}}{3kT} = 8\phi\epsilon$ grows linearly in ϕ we arrive at

$$\frac{M(\alpha)}{M_{sat}} = L_{0,0} + \phi \sum_{n=1}^{\infty} L_{1,n}\epsilon^n + O(\phi^2) \tag{4.24a}$$

with

$$L_{0,0} = \mathcal{L}(\alpha) \tag{4.24b}$$

$$L_{1,1} = 8\mathcal{L}(\alpha)\mathcal{L}'(\alpha) \tag{4.24c}$$

$$L_{1,n} = G_n'(\alpha) \qquad \text{for} \qquad n \geq 2 \; . \tag{4.24d}$$

This is a consistent approximation in terms of ϕ. On the other hand, solving Eq. (4.22) in a formally exact manner for M would introduce higher orders in ϕ which we already neglected to arrive at Eq. (4.22).

Note also that $M_{sphere}(\alpha_s)/M_{sat}$ (4.21) contains *explicitly* a term $\sim \phi\epsilon^2$ as lowest non-trivial power coming from the expansion in the near-field dipolar coupling strength. On the other hand the self-consistent solution (4.24) that solves Eq. (4.22) starts out with a contribution $\sim \phi\epsilon$. The latter arises from the far-field dipolar continuum via the magnetization M in the dipole-induced shift of the argument, $\alpha + \frac{mM}{3kT}$, of the Langevin function in Eq. (4.22)

— in the absence of any dipolar interactions in the system one would have $H_s = H_e = H$ leading to ideal paramagnetism.

D. Comparison with previous results

The Onsager model, the Weiss model, and our calculation agree that up to order $\phi\epsilon$

$$\frac{M}{M_{sat}} = \mathcal{L}(\alpha) + 8\phi\epsilon\mathcal{L}(\alpha)\mathcal{L}'(\alpha) + O(\phi^2) + O(\epsilon^2) \quad . \tag{4.25}$$

This expression was also derived by Buyevich and Ivanov [22] with a calculation similar to ours. However, they did not introduce a magnetic continuum approximation. Instead, they assumed a special probe geometry of a long cylinder parallel to the external magnetic field and performed an integration over all the particle's dipolar fields in the cylinder explicitly. The magnetization was therefore given in terms of the external field. Their result agrees with ours because for the cylindrical geometry chosen in [22] $\mathbf{H}_e$ equals $\mathbf{H}$.

A second paper that deals with our problem in a similar way was published by Kalikmanov [34]. In section 4, the author arrives at an equation for the magnetization that reads in our notation

$$\frac{M}{M_{sat}} = \mathcal{L}(\alpha) + 3\phi\epsilon^2 G_2'(\alpha)\int_1^\infty \frac{g_0(x)}{x^4}dx \quad . \tag{4.26}$$

Here $g_0(x)$ is the hard sphere correlation function. In our $O(\phi)$–approximation this function has to be set to one. Then the $\phi\epsilon^2$–term agrees with ours. Note, however, that the above result (4.26) of Kalikmanov does not contain the $\phi\epsilon$–term resulting from the magnetic field from the continuum.

V. EXPANSION UP TO SECOND ORDER IN ϕ AND ϵ

It is possible to calculate $O(\phi^2)$–terms of the Born–Mayer expansion when ϵ is taken into account up to second order only. A more elegant way to calculate the magnetization in this approximation makes use of the grand canonical rather than the canonical ensemble. This

approach allows to avoid the determination of some terms that can be factorized into already known integrals and cancel out in the calculation of the free energy. However, the grand canonical approach has the disadvantage that it yields the magnetization as function of the chemical potential μ rather than the particle number N. Some more algebra is then required to find out the function $\mu(N)$. Here we continue to work with the canonical ensemble.

A. The graphs

Figure 3 shows the 12 additional graphs that are of second order in ϕ and of less than third order in ϵ. Four of them vanish because they contain at least one first–order dipolar interaction term between otherwise unrelated particles. Integration over the relative position of these particles while leaving the relative positions between all other particles and the direction of the magnetic moments fixed yields zero since it involves a spatial averaging over a dipolar field. The graph labelled with the letter F vanishes for similar reasons that are explained in Appendix B where we calculate the integrals one by one. Their respective contribution to the partition function is

$$Z_A/Z_0 = 32N\phi^2 \tag{5.1a}$$

$$Z_B/Z_0 = -16N\phi^2\epsilon^2 G_2(\alpha_s) \tag{5.1b}$$

$$Z_C/Z_0 = 8(N^2 - 6N)\phi^2 \tag{5.1c}$$

$$Z_D/Z_0 = -4(N^2 - 6N)\phi^2\epsilon^2 G_2(\alpha_s) \tag{5.1d}$$

$$Z_E/Z_0 = -5N\phi^2 \tag{5.1e}$$

$$Z_F/Z_0 = 0 \tag{5.1f}$$

$$Z_G/Z_0 = \frac{1 + 6\ln 2}{4} N\phi^2\epsilon^2 G_2(\alpha_s) \tag{5.1g}$$

$$Z_H/Z_0 = -N\phi^2\epsilon^2 K(\alpha_s) \ . \tag{5.1h}$$

The functions G_2 and K are given in Appendix A.

B. Free energy and magnetization

Now we have all necessary terms at hand to calculate the canonical partition function up to the desired order:

$$\begin{aligned}\frac{Z}{Z_0} &= 1-4(N-1)\phi+(N-1)\phi\epsilon^2 G_2(\alpha_s)\\ &+32N\phi^2-16N\phi^2\epsilon^2G_2(\alpha_s)+8(N^2-6N)\phi^2\\ &-4(N^2-6N)\phi^2\epsilon^2G_2(\alpha_s)-5N\phi^2\\ &+\frac{1+6\ln 2}{4}N\phi^2\epsilon^2G_2(\alpha_s)-N\phi^2\epsilon^2K(\alpha_s)+H.O.T.\ .\end{aligned} \tag{5.2}$$

The terms in $O(\phi)$ appear already in (4.17). They are presented here including the next higher order in N. The other terms come from Z_A – Z_H. To include all terms of $O(\phi^2,\epsilon^2)$ in the free energy one has to approximate the logarithm $\ln(1+x)$ by $x-x^2/2$. The quadratic order is necessary only for the $O(\phi)$–terms. New terms of $O(N^2)$ appear and cancel against those of the terms from Z_C and Z_D. One gets

$$\begin{aligned}\frac{F}{kT} &= -N\ln z_0+4N\phi+5N\phi^2\\ &-N\phi\epsilon^2G_2(\alpha_s)-\frac{1+6\ln 2}{4}N\phi^2\epsilon^2G_2(\alpha_s)\\ &+N\phi^2\epsilon^2K(\alpha_s)+H.O.T.\ .\end{aligned} \tag{5.3}$$

The result is proportional to N as it has to be.

The magnetization of the sphere is

$$\begin{aligned}\frac{M_{sphere}(\alpha_s)}{M_{sat}} &= \mathcal{L}(\alpha_s)+\phi\epsilon^2G_2'(\alpha_s)\\ &+\frac{1+6\ln 2}{4}\phi^2\epsilon^2G_2'(\alpha_s)-\phi^2\epsilon^2K'(\alpha_s)+H.O.T.\ .\end{aligned} \tag{5.4}$$

To calculate the magnetization as a function of α we identify (5.4) with M and use again $\alpha_s=\alpha+\frac{mM}{3kT}$. The right hand side of (5.4) has now to be expanded around α up to second order and the resulting equation has to be iterated twice to take into account all important terms up to $\epsilon^2\phi^2$. The result is

$$\frac{M(\alpha)}{M_{sat}} = L_{0,0} + \phi\epsilon L_{1,1} + \phi\epsilon^2 L_{1,2} + \phi^2\epsilon^2 L_{2,2} + ... \tag{5.5a}$$

with $L_{0,0}, L_{1,1}$, and $L_{1,2}$ defined in eqs. (4.24b) - (4.24d) and

$$\begin{aligned} L_{2,2} = {} & 64\mathcal{L}(\alpha)\mathcal{L}'(\alpha)^2 + 32\mathcal{L}(\alpha)\mathcal{L}''(\alpha) \\ & + \frac{1+6\ln 2}{4} G_2'(\alpha) - K'(\alpha) \; . \end{aligned} \tag{5.5b}$$

For the discussion in the next Sec. we decompose

$$L_{2,2}(\alpha) = L_{2,2}^{sphere}(\alpha) + L_{2,2}^{iterative}(\alpha) \; . \tag{5.6a}$$

The function

$$L_{2,2}^{sphere} = \frac{1+6\ln 2}{4} G_2' - K' \tag{5.6b}$$

occurs already in the expression (5.4) for the magnetization $M_{sphere}(\alpha_s)$ of the sphere. The contribution

$$L_{2,2}^{iterative} = 64\mathcal{L}(\mathcal{L}')^2 + 32\mathcal{L}\mathcal{L}'' \tag{5.6c}$$

arises in obtaining the selfconsistent solution of the equation $M = M_{sphere}$ with an expansion and iteration.

VI. DISCUSSION OF THE RESULTS

We will first show that our result (5.4) for $M_{sphere}(H_s)$ does not lead to a ferromagnetic solution in contradistinction to the Weiss model. Then we discuss the behavior of the different terms contributing to (4.24) and to (5.5) and we delineate the range of reliability of the simplest approximation. Finally, we address problems arising when comparing with experiments.

A. Spontaneous magnetization?

Investigations based on density functional methods by Groh and Dietrich [4] and on Monte Carlo methods by Weis and Levesque [8,9] provided support for the existence of magnetized phases for absent *external* field H_e, i. e., ferromagnetism, in the system of dipolar hard spheres we consider in this work. Groh and Dietrich consider a ferrofluid probe of needle–like shape where $H = H_e$ and find a transition to a magnetized phase at $\phi\epsilon \approx 0.35$. But they consider this value as being overestimated and refer to [9]. Weis and Levesque study a case without demagnetizing fields, i. e., again $H = H_e$. They find a transition to a magnetized phase at $\epsilon = 6.25$ for $\phi \approx 0.35$. As discussed in detail below, these values are outside the range of reliability of our results.

The Weiss model does also show ferromagnetic behavior. It is recovered from (5.4) by keeping only the leading–order term $\mathcal{L}(\alpha_s)$ describing a single moment in the field $H_s = H + M/3$. The resulting self–consistency equation

$$M = M_{sphere}^{Weiss}\left(H + \frac{M}{3}\right) = M_{sat}\mathcal{L}\left[\frac{m}{kT}\left(H + \frac{M}{3}\right)\right] \tag{6.1}$$

allows for zero field a solution with finite magnetization when $kT < mM_{sat}/9$. Using (2.4) combined with (2.12) and (2.13) this condition is equivalent to $\phi\epsilon > 3/8$, about the same value as in [4]. So according to the Weiss model the ferrofluid will show ferromagnetic behavior below a critical temperature that grows linearly with the saturation magnetization M_{sat} of the ferrofluid. But even for a ferrofluid consisting of cobalt particles with a magnetic core diameter of 10 nm and a magnetic volume fraction of $\phi_{mag} = 0.1$ the critical temperature would be as low as 90 K.

While the transition combination $\epsilon = 6.25$, $\phi \approx 0.35$ of [9] is outside the range of reliability of our results, the threshold location $\phi\epsilon = 8/3$ of the Weiss model may be not. However, in agreement with [9] we do not find selfconsistent ferromagnetic solutions of the equation (5.4) $M = M_{sphere}(H + M/3)$ within this range. We have numerically confirmed that for $H = 0$ the equation $M = M_{sphere}(M/3)$ allows *always* only the trivial solution $M = 0$.

B. Contribution from different orders

Now we will take a closer look on the functions of α involved in (4.24) and (5.5). All these functions are odd as it has to be for reasons of symmetry. For $\alpha \to \infty$ they vanish as $1/\alpha^2$ or faster. Because $1 - \mathcal{L}(\alpha) \sim 1/\alpha$ that means that the predicted magnetization is always smaller than the saturation magnetization for $\alpha \to \infty$. Nevertheless the magnetization can assume unphysical values $> M_{sat}$ for intermediate α if ϵ or ϕ is big enough for the approximations to become invalid.

1. Behavior in linear order of ϕ

We will first discuss the result (4.24) for the magnetization that was obtained up to linear order in the volume fraction ϕ. In figure 4 the functions $L_{1,1}$ and $L_{1,2}$ are plotted. The values of the higher–order functions are smaller, but their shape remains more or less the same as the logarithmic plot in figure 5 shows. Because $L_{1,n}$ and $L_{1,n+2}$ differ by about one order of magnitude one can conclude that by including higher and higher orders of ϵ the series (5.5) for the magnetization converges, as long as ϵ is smaller than ≈ 3. For this large value of ϵ strong agglomeration can already be expected.

For small α, $L_{1,n}$ is proportional to α (α^3) for odd (even) n. The initial susceptibility can therefore be written as

$$\chi(H=0) = \chi_0(H=0)\left[1 + \phi \sum_{n=0} s_{1,2n+1}\epsilon^{2n+1} + O(\phi^2)\right] \quad . \tag{6.2}$$

Here

$$\chi_0(H=0) = \frac{mM_{sat}}{3kT} \quad , \tag{6.3}$$

is the initial susceptibility of the ideal paramagnetic gas, and the nonvanishing $s_{1,n}$ we calculated are

$$s_{1,1} = \frac{8}{3}; \qquad s_{1,3} = \frac{8}{75}; \qquad s_{1,5} = \frac{32}{3675}$$
$$s_{1,7} = \frac{8}{19845}; \qquad s_{1,9} = \frac{148}{12006225} \ . \tag{6.4}$$

Figure 6 shows $\chi_0(H = 0)$ (thick dashed line), and the susceptibility $\chi(H = 0)$ (6.2) including progressive orders $\phi\epsilon$, $\phi\epsilon^3$, $\phi\epsilon^5$, $\phi\epsilon^7$, and $\phi\epsilon^9$ (thin dashed lines, from bottom to top) as a function of ϵ for $\phi = 0.15$. The sequence of these thin dashed lines shows that this series converges in the ϵ–range of figure 6. The last thick full line in Figure 6 represents $\chi(H = 0)$ including the contributions in order $\phi^2\epsilon^2$. It shows that the latter are even for $\phi = 0.15$ not yet important.

2. Behavior in second order of ϕ

Now we take a look at the functions $L_{2,2}^{sphere}$ (5.6b) and $L_{2,2}^{iterative}$ (5.6c) that add up to $L_{2,2}$ (5.6a) which enters in order $\phi^2\epsilon^2$ into the magnetization (5.5a).

Figure 7 shows that the contributions $L_{2,2}^{sphere}$ and $L_{2,2}^{iterative}$ almost cancel each other at small α. This is why the influence of the $\phi^2\epsilon^2$–terms on the susceptibility in figure 6 is so small. However, at higher α the $\phi^2\epsilon^2 L_{2,2}$–term becomes important. Comparing the latter with the linear one, $\phi\epsilon L_{1,1}$, one finds that they contribute for $\epsilon\phi \approx 0.5$ equally at larger α.

Except for very small α $L_{2,2}$ is negative, because it includes higher–order particle position correlations that result in a better modeling of the distance distribution due to the finite size of the particles. The mean distance is bigger in this approximation and the induced dipolar fields at the particle positions are therefore smaller.

The influence of the $\phi^2\epsilon^2 L_{2,2}$ contribution to the magnetization is shown in figure 8 for $\epsilon = 2$ and $\phi = 0.05$. For these parameters this term is already large enough to cancel almost exactly the sum of all contributions $L_{1,n}\phi\epsilon^n$, with $n \geq 2$ from the linear order in ϕ at moderate α. Figure 9 shows the susceptibility $\chi(H) = \frac{\partial M(H)}{\partial H}$ for the same parameters. At higher α, the cancellation of the higher $L_{1,n}$–terms against the $L_{2,2}$–contribution can again be seen. At smaller α, however, the behavior is different. There the contribution of the

$L_{1,n}$–terms is much larger, whereas the $L_{2,2}$–contributions vanish.

C. Reliability of the $O(\phi\epsilon)$–approximation

We can determine the range of reliability of the simplest approximation

$$\begin{aligned}\frac{M}{M_{sat}} &= L_{0,0}(\alpha) + L_{1,1}(\alpha)\phi\epsilon \\ &= \mathcal{L}(\alpha) + 8\mathcal{L}(\alpha)\mathcal{L}'(\alpha)\phi\epsilon \end{aligned} \tag{6.5}$$

to the magnetization that includes effects of dipolar interactions since we know the higher–order corrections in ϕ as well as in ϵ. To that end we investigated the ratios

$$\left| \frac{O(\phi\epsilon^n)\text{–terms } (n>1)}{L_{0,0}(\alpha) + L_{1,1}(\alpha)\phi\epsilon} \right| \quad , \tag{6.6}$$

and

$$\left| \frac{O(\phi^2)\text{–terms}}{L_{0,0}(\alpha) + L_{1,1}(\alpha)\phi\epsilon} \right| \quad . \tag{6.7}$$

The first ratio assumes its maximum at $\alpha = 0$, that means the initial susceptibility is most sensitive to higher order corrections in ϵ. The second ratio (6.7) assumes its maximum around $\alpha = 2$, that is near the maximum of the absolute value of the numerator (as seen in figure 7).

In the ϵ–ϕ plane of figure 10(a) we show isolines of the maximal – with respect to α – ratio (6.6) and figure 10(b) shows the analogous isolines for the ratio (6.7). The comparison shows that the smallness of ϵ is more important to keep the ratio (6.6) small, whereas in (6.7) the value of ϕ is also important. As rules of thumb one can say that the approximation (6.5) is valid within about 1 – 2 percent if $\epsilon < 1$ and $\epsilon\phi < 0.04$. If the first constraint is not fulfilled, higher orders in ϵ have to be taken into account. Higher orders in ϕ are needed if the second constraint is not fulfilled.

D. Comparison with experiments?

There are several papers [23–26] that aim at investigating the influence of dipolar interactions on the magnetization by comparing theoretical models developed so far with experimental magnetizations of ferrofluids. The mean spherical model [21] was reported to show good agreement with experiments. Pshenichnikov [23] found also good agreement with the high temperature approximation [22], i. e., the approximation (6.5). But this ansatz failed in the magneto–granulometric analysis done in [26].

We do not present a comparison of our results with the experiments on the magnetization in the literature because of several problems: In our theory it is necessary to distinguish between the particle diameter D and the magnetic core diameter D_{mag} that is found in magneto–granulometric measurements. This problem does not arise in the mean spherical model or the high temperature approximation, where ϵ and ϕ enter only via the factor $\phi\epsilon = \frac{Nm^2}{24V\mu_0 kT} = \frac{M_{sat}m}{24kT}$ that is independent of D. Also, corrections such as the temperature dependence of the saturation magnetization or the fluid density should be taken into account [25].

But the major problem in comparing directly with experiments is that our theory does not take into account the polydispersity of ferrofluids. The effect of polydispersity is significant already in the absence of any dipolar interaction. This can be inferred from the dashed and the dotted curves in Fig. 11 representing the reduced magnetization of *noninteracting* magnetic particles having a polydisperse and a monodisperse distribution of particle diameters, respectively. Here the common particle diameters of the latter is $\overline{D^3}^{1/3}$, where $\overline{D^3}$ is the third moment of the particle size distribution

$$P(D) := \frac{1}{\sqrt{2\pi}\sigma D_0 e^{\sigma^2/2}} e^{-\frac{\ln^2 D/D_0}{2\sigma^2}} \quad . \tag{6.8}$$

of the former. The mean magnetic moment $\overline{m}$ and the saturation magnetization of the two systems are the same. For comparison with the effect of dipolar interaction in *monodisperse* systems the full curve in Fig. 11 shows our result for M (5.5a) including all terms $\sim \phi\epsilon^n$

and the term $\phi^2\epsilon^2$. Hence the effects of polydispersiveness alone, i. e., without interaction are comparable in size with the effect of dipolar interactions in monodisperse systems. Thus clearly an extension of the here presented Born–Mayer expansion method to the case of polydisperse interacting particles is desirable.

VII. CONCLUSION

We calculated the free energy and in particular the magnetization M of a ferrofluid as a function of the macroscopic magnetic field H. To do so, we used the technique of the Born–Mayer expansion together with an expansion in terms of the dipolar coupling energy. The magnetic particles were assumed to be hard spheres with a common hard core diameter D and magnetic moment m that interact via long range dipolar interactions. This feature may result in a geometry dependence of thermodynamic properties. We treated this problem by dividing the dipolar field at some position $\mathbf{x}_i$ that is produced by the magnetic moments of the particles into a near–field and into a far–field part depending on whether the particle distance from $\mathbf{x}_i$ is larger than some radius R_s or not. In this way *every* magnetic particle is imagined to be located in the center of a sphere of radius R_s. The far–field dipolar contribution from particles beyond R_s is then replaced by a magnetic continuum with magnetization M and magnetic field H. Here R_s is chosen to be such that M and H are homogeneous on the scale of R_s. The magnetic continuum outside the sphere produces in the center of the sphere the magnetic field $H_s = H + M/3$. This field acts as an "external" field on the particle in the center of the sphere. The near–field interaction of the latter with the other particles within the sphere being at a distance smaller than R_s is treated explicitly. Thus in our statistical mechanical calculations there appear dipolar interactions only with interparticle distances less than R_s. However, since the cutoff dependence of the relevant expressions occurring in these calculations is negligible already beyond a radius of the order of $10D \approx 100$ nm we used $R_s = \infty$ in these expressions.

The expansion of the partition function for these interacting particles in terms of the

volume ratio and the dipolar coupling strength ϵ yields an expression for the magnetization

$$M_{sphere} = M_{sphere}(H + M/3) \ . \tag{7.1}$$

as a function of the "external" part of the field inside the sphere. The magnetization M_{sphere} is then identified with the magnetization $M(H)$ inside the continuum so that a selfconsistent relation results. The aforementioned geometry dependence of M in the general case is incorporated via H.

We presented two different expansions in ϵ and ϕ, one containing only linear terms in ϕ, the other also second order ϕ terms, but only up to $O(\epsilon^2)$. We discussed the range of applicability in the ϕ–ϵ plane of their results for $M(H)$ and compared them to the most simple approximation to the magnetization that contains the dipolar effects only in linear order in ϵ and ϕ. The selfconsistent relation for $M(H)$ that contains only up to second order terms in both parameters does not admit a ferromagnetic solution with spontaneous magnetization. Finally we showed that an extension to polydisperse interacting particles is desirable.

ACKNOWLEDGMENTS

This work was supported by the Deutsche Forschungsgemeinschaft (SFB 277).

APPENDIX A: THE FUNCTIONS G_n AND K

The functions $G_n^*(x)$ in (4.13) are related to $G_n(x)$ via (4.18):

$$G_n(x) = \frac{1}{16\pi^3(n-1)n!}\left(\frac{x}{\sinh x}\right)^2 G_n^*(x) \ . \tag{A1}$$

The functions $G_n(x)$ introduced in (4.18) have the form

$$\begin{aligned} G_n(x) = G_n^{(0)}\left(\frac{1}{x}\right) + G_n^{(1)}\left(\frac{1}{x}\right)\coth x \\ + G_n^{(2)}\left(\frac{1}{x}\right)\coth^2 x \ , \end{aligned} \tag{A2}$$

where the functions $G_n^{(i)}(y)$ are polynomials. The first four triple are given by

$$G_2^{(0)}(y) = \frac{8}{5} + \frac{8}{5}y^2 + \frac{12}{5}y^4 \tag{A3a}$$

$$G_2^{(1)}(y) = -\frac{8}{5}y - \frac{24}{5}y^3 \tag{A3b}$$

$$G_2^{(2)}(y) = \frac{12}{5}y^2 \tag{A3c}$$

$$G_3^{(0)}(y) = -\frac{4}{35}y^2 - \frac{48}{35}y^4 - \frac{12}{7}y^6 \tag{A4a}$$

$$G_3^{(1)}(y) = -\frac{8}{35}y + \frac{8}{5}y^3 + \frac{24}{7}y^5 \tag{A4b}$$

$$G_3^{(2)}(y) = \frac{16}{105} - \frac{8}{35}y^2 - \frac{12}{7}y^4 \tag{A4c}$$

$$G_4^{(0)}(y) = \frac{8}{105} + \frac{8}{35}y^2 + \frac{92}{35}y^4 + \frac{72}{7}y^6 + 12y^8 \tag{A5a}$$

$$G_4^{(1)}(y) = -\frac{16}{105}y - \frac{8}{5}y^3 - \frac{88}{7}y^5 - 24y^7 \tag{A5b}$$

$$G_4^{(2)}(y) = \frac{32}{105}y^2 + \frac{16}{7}y^4 + 12y^6 \tag{A5c}$$

$$G_5^{(0)}(y) = \frac{12}{385}y^2 - \frac{208}{385}y^4 - \frac{852}{77}y^6 - \frac{480}{11}y^8 - \frac{540}{11}y^{10} \tag{A6a}$$

$$G_5^{(1)}(y) = -\frac{8}{231}y + \frac{16}{385}y^3 + \frac{472}{77}y^5 + \frac{600}{11}y^7 + \frac{1080}{11}y^9 \tag{A6b}$$

$$G_5^{(2)}(y) = \frac{16}{1155} + \frac{16}{1155}y^2 - \frac{40}{77}y^4 - \frac{120}{11}y^6 - \frac{540}{11}y^8 \quad . \tag{A6c}$$

All functions $G_n^{(i)}(x)$ have a well defined limit for $x \to 0$ although this is not obvious for the above explicit expressions. Their values at $x = 0$ are closely related to the coefficients in the ϵ–expansion of the second virial coefficient for the system of dipolar hard spheres in the absence of a magnetic field. The calculation of this coefficient dates back to [35] and can also be found in [36].

The function K (B22) that appears in the $O(\phi^2)$–terms of the free energy is given by

$$K(x) = -\frac{6}{x}\coth^3 x + \left(\frac{18}{x^2} + 12\right)\coth^2 x - \left(\frac{18}{x^3} + \frac{24}{x}\right)\coth x + \frac{6}{x^4} + \frac{12}{x^2} \quad . \tag{A7}$$

APPENDIX B: GRAPHS IN SECOND ORDER OF ϕ

Here we determine the contribution to the canonical partition function from the graphs A–H shown in Fig. 3. There often appear hard core interaction terms that are just expressions of the requirement that two particles have to or must not overlap. We define two abbreviations:

$$e^{-v_{ij}^{HC}} - 1 = -O_{ij} \quad , \tag{B1}$$

$$e^{-v_{ij}^{HC}} = \overline{O}_{ij} \quad . \tag{B2}$$

1. Graph A

The graph A represents $f_{ij}^{(0)} f_{ik}^{(0)}$. There are N^3 ways to choose the constituting particles. But because j and k are equivalent only $N^3/2$ distinctive graphs remain. Integration over all variables except the positions of particle j and k relative to i yields

$$\frac{N^3}{2} \int f_{12}^{(0)} f_{13}^{(0)} \prod_l e^{-v_l} \, d\,\vec{\mathbf{x}} \, d\,\vec{\Omega}$$
$$= \frac{N^3}{2} \left(4\pi \frac{\sinh \alpha_s}{\alpha_s}\right)^N V^{N-2} \int O_{12} O_{13} d\mathbf{r}_{12} d\mathbf{r}_{13} \quad .$$

The remaining integral factorizes and we can make use of the results for A_0 (4.9). The contribution of graph A to the partition function is

$$Z_A = 32 N Z_0 \phi^2 \tag{B3}$$

where Z_0 is given by (4.4).

2. Graph B

The graph B represents $f_{ij}^{(0)} f_{ik}^{(2)}$. All three particles appear in different ways, thus there are N^3 different graphs. After integration over the degrees of freedom of the noninvolved particles and switching to relative coordinates with respect to particle i the integral factorizes again and one can make use of the results for A_0 (4.9) and A_2 (4.14). We get

$$Z_B = -16 N Z_0 \phi^2 \epsilon^2 G_2(\alpha_s) \ . \tag{B4}$$

3. Graph C

The graph C represents $f_{ij}^{(0)} f_{kl}^{(0)}$. Here we have also to include the next higher order term when we calculate the number of combinations to get the $O(N)$–terms in the final result: There are $(N^4 - 6N^3)/8$ different terms. The integral for graph C can be factorized so that

$$Z_C = 8(N^2 - 6N) Z_0 \phi^2 \ . \tag{B5}$$

4. Graph D

The graph D represents $f_{ij}^{(0)} f_{kl}^{(2)}$. The calculation is similar to the calculation of graph C. Again, we need the next higher order term in N. There are $(N^4 - 6N^3)/4$ combinations, twice as much as for graph C because the pairs (i, j) and (k, l) are not identical. One gets

$$Z_D = -4(N^2 - 6N) Z_0 \phi^2 \epsilon^2 G_2(\alpha_s) \ . \tag{B6}$$

5. Graph E

The integral containing the term $f_{ij}^{(0)} f_{jk}^{(0)} f_{ki}^{(0)}$ is the first really new integral. It involves only hard core interactions and does not contribute to the final expression for the magnetization. But for completeness we will calculate it also. The trivial integrations yield

$$Z_E = -\frac{N^3}{6}\left(4\pi\frac{\sinh\alpha_s}{\alpha_s}\right)^N V^{N-2}\int O_{12}O_{13}O_{23}d\mathbf{r}_{12}d\mathbf{r}_{13} \quad . \tag{B7}$$

We keep the distance $\mathbf{r}_{12}$ fixed. The center of particle 3 has then to be inside two spheres of radius D around particle 1 and 2. Integrating over the position of particle 3 yields the overlap volume V_o of the two spheres

$$V_o = \frac{4}{3}\pi D^3\left[1-\frac{3}{4}\frac{r_{12}}{D}+\frac{1}{16}\left(\frac{r_{12}}{D}\right)^3\right] \quad . \tag{B8}$$

Therefore

$$\begin{aligned} Z_E &= -\frac{N^3}{6}\frac{Z_0}{V^2}\int O_{12}V_o(r_{12})d\mathbf{r}_{12} \qquad (B9)\\ &= -\frac{N^3}{6}\frac{Z_0}{V^2}4\pi\int_0^D V_o(r_{12})r_{12}^2dr_{12} \quad . \end{aligned}$$

Performing the last integration results in

$$Z_E = -5NZ_0\phi^2 \quad . \tag{B10}$$

6. Graph F

The graph F represents $f_{ij}^{(0)}f_{ik}^{(0)}f_{jk}^{(1)}$. As already stated this integral vanishes which can be seen as follows: Consider an arbitrary configuration belonging to some value of the integrand

$$e^{-v_i-v_j-v_k}f_{ij}^{(0)}f_{ik}^{(0)}f_{jk}^{(1)} \quad . \tag{B11}$$

While leaving the direction of the magnetic moments fixed the whole configuration can be freely rotated around particle j changing only the $f_{jk}^{(1)}$ term. Integration over the resulting configurations involves again an averaging over a dipolar field on a spherical surface.

7. Graph G

The calculation of the $N^3/2$ integrals belonging to $f_{ij}^{(0)}f_{ik}^{(0)}f_{jk}^{(2)}$ is similar to the calculation for graph E. First we integrate over all degrees of freedom except the distance between particle $j=1$ and $k=2$ and the position of particle $i=3$:

$$Z_G = \frac{N^3}{2}\left(4\pi\frac{\sinh\alpha_s}{\alpha_s}\right)^N V^{N-2}\pi G_2(\alpha_s)\epsilon^2 D^6 \times \int O_{13}O_{23}\overline{O}_{12}r_{12}^{-4}dr_{12}d\mathbf{r}_3 \ . \tag{B12}$$

Integrating over $\mathbf{r}_3$ results again in an overlap volume term:

$$Z_G = \frac{N^3}{2}\frac{Z_0}{V^2}\pi G_2(\alpha_s)\epsilon^2 D^6 \int \overline{O}_{12}V_o(r_{12})r_{12}^{-4}dr_{12} \ . \tag{B13}$$

Here the lower integration boundary is $r_{12} = D$ because of the remaining hard core factor. The upper integration boundary is $r_{12} = 2D$ because the possibility that particle 3 overlaps with particle 1 and 2 is still required. The final result is

$$Z_G = \frac{1+6\ln 2}{4}NZ_0\phi^2\epsilon^2 G_2(\alpha_s) \ . \tag{B14}$$

8. Graph H

The last graph H is the most complicated one. It represents the term $f_{ij}^{(0)}f_{ik}^{(1)}f_{jk}^{(1)}$ that appears $N^3/2$ times. The problem here is to fulfill the requirement that particles j and k have to overlap in terms of properly chosen integration limits. We start with performing the trivial integrations:

$$Z_H = -\frac{1}{2}N^3 z_0^{N-3}V \times \int e^{-v_1-v_2-v_3}v_{12}^{DD}v_{13}^{DD}O_{23}\overline{O}_{12}\overline{O}_{13} \times d\mathbf{r}_{12}d\mathbf{r}_{13}d\Omega_1 d\Omega_2 d\Omega_3 \ . \tag{B15}$$

Whether the integrand vanishes due to the hard core factors depends only on the distances r_{12}, r_{13}, and the angle ϑ_{23} between $\mathbf{r}_{12}$ and $\mathbf{r}_{13}$. Consider a special orientation where

$$\hat{\mathbf{r}}_{12}^0 = (1,0,0) \tag{B16}$$

$$\hat{\mathbf{r}}_{13}^0 = (\cos\vartheta_2, 0, \sin\vartheta_{23}) \ , \tag{B17}$$

with $0 \le \vartheta_{23} \le \pi$. A general configuration of the particles' locations can be written as

$$\hat{\mathbf{r}}_{1(2,3)} = \mathcal{R}_z(\varphi)\mathcal{R}_y(\vartheta)\mathcal{R}_z(\psi)\hat{\mathbf{r}}^0_{1(2,3)} \quad , \tag{B18}$$

where $\mathcal{R}_x$, $\mathcal{R}_y$, and $\mathcal{R}_z$ are Eulerian rotation matrices for the angles ψ, ϑ, and φ. Using this form the integration over the factors that depend on these angles:

$$\int_0^{2\pi}\int_{-\pi/2}^{\pi/2}\int_0^{2\pi} v_{12}^{DD} v_{13}^{DD} \cos\vartheta d\varphi d\vartheta d\psi \quad , \tag{B19}$$

can easily be performed with *mathematica*. We call the result $I(r_{12}, r_{13}, \vartheta_{23}, \mathbf{m}_i)$.

Next, we integrate over the orientations of the $\mathbf{m_i}$:

$$\int e^{-v_1-v_2-v_3} I(r_{12}, r_{13}, \vartheta_{23}, \mathbf{m}_i) d\Omega_1 d\Omega_2 d\Omega_3 \quad . \tag{B20}$$

The result depends only on r_{12}, r_{13}, and ϑ_{23}. Using it in (B15) yields

$$\begin{aligned} Z_H = &-\frac{4}{3}N^3\frac{Z_0}{V^2}K(\alpha_s) \\ &\times \int O_{23}\overline{O}_{12}\overline{O}_{13}\frac{m^4\pi^2(2\cos^2\vartheta_{23} - \sin^2\vartheta_{23})}{10(4\pi\mu_0 kT)^2 r_{12} r_{13}} \\ &\times \sin\vartheta_{23} dr_{12} dr_{13} d\vartheta_{23} \quad , \end{aligned} \tag{B21}$$

where

$$\begin{aligned} K(\alpha_s) = &\frac{3}{8}\left(\frac{\alpha_s}{\sinh\alpha_s}\right)^3 \int_{-1}^{1}\int_{-1}^{1}\int_{-1}^{1} e^{\alpha_s(u_1+u_2+u_3)} \\ &\times (u_1^2+3) u_2 u_3 du_1 du_2 du_3 \quad . \end{aligned} \tag{B22}$$

The explicit expression for $K(\alpha_s)$ is given in Appendix A (eqn. A7).

Now we discuss the hard core terms. r_{12} and r_{13} have to be greater than D to avoid the overlap with particle 1. Furthermore $|r_{12} - r_{13}| < D$ has to be fulfilled for particle 2 and 3 to overlap. As a last requirement, ϑ_{23} has to be smaller than some angle $\vartheta_{23}^{\max}$ that depends on r_{12} and r_{13}. Trigonometry shows that

$$\cos\vartheta_{23}^{\max} = \frac{r_{12}^2 + r_{13}^2 - D^2}{2 r_{12} r_{13}} \quad . \tag{B23}$$

In this configuration the distance between particle 2 and 3 is exactly D.

We perform the integration over ϑ_{23} from 0 to $\vartheta_{23}^{\max}$ in (B21), choose the correct limits for r_{12} and r_{13}, and drop all hard core terms:

$$
\begin{aligned}
Z_H = & -\frac{4}{3} N^3 \frac{Z_0}{V^2} K(\alpha_s) \\
& \times \int_D^\infty \int_{\min(D, r_{13}-D)}^{r_{13}+D} \frac{m^4 \pi^2}{10 (4\pi\mu_0 kT)^2 r_{12} r_{13}} \\
& \times \left[\frac{r_{12}^2 + r_{13}^2 - D^2}{2 r_{12} r_{13}} - \left(\frac{r_{12}^2 + r_{13}^2 - D^2}{2 r_{12} r_{13}} \right)^3 \right] dr_{12} dr_{13} \quad ,
\end{aligned}
\tag{B24}
$$

The result of the last integration is:

$$
\begin{aligned}
Z_H &= -\frac{4}{3} N^3 \frac{Z_0}{V^2} K(\alpha_s) \frac{m^4 \pi^2}{48 (4\pi\mu_0 kT)^2} \\
&= -N Z_0 \phi^2 \epsilon^2 K(\alpha_s) \quad .
\end{aligned}
\tag{B25}
$$

REFERENCES

[1] R. E. Rosensweig, *Ferrohydrodynamics*, (Cambridge University Press, Cambrigde, United Kingdom, 1985)

[2] B. Groh and S. Dietrich, Phys. Rev. Lett. **72**, 2422 (1994).

[3] B. Groh and S. Dietrich, Phys. Rev. E **53**, 2509 (1996)

[4] B. Groh and S. Dietrich, Phys. Rev. E **55**, 2892 (1997)

[5] B. Groh and S. Dietrich, Phys. Rev. Lett. **79**, 749 (1997)

[6] B. Groh and S. Dietrich, Phys. Rev. E **57**, 4535 (1998).

[7] M. E. van Leeuwen and B. Smit, Phys. Rev. Lett. **71**, 3991 (1993).

[8] J. J. Weis and D. Levesque, Phys. Rev. Lett. **71**, 2729 (1993).

[9] J. J. Weis and D. Levesque, Phys. Rev. E **48**, 3728 (1993).

[10] M- J. Stevens and G. S. Grest, Phys. Rev. E **51**, 5962 (1995).

[11] M- J. Stevens and G. S. Grest, Phys. Rev. E **51**, 5976 (1995).

[12] J. C. Shelley, G. N. Patey, D. Levesque, and J. J. Weis, Phys. Rev. E **59**, 3065 (1999).

[13] J. M. Tavares, J. J. Weis, and M. M. Telo da Gama, Phys. Rev. E **59**, 4388 (1999).

[14] P. J. Camp, J. C. Shelley, and G. N. Patey, Phys. Rev. Lett. **84**, 115 (2000).

[15] R. P. Sear, Phys. Rev. Lett. **76**, 2310 (1996).

[16] R. van Roij, Phys. Rev. Lett. **76**, 3348 (1996).

[17] J. M. Tavares, M. M. Telo da Gama, and M. A. Osipov, Phys. Rev. E **56**, R6252 (1997).

[18] Y. Levin, Phys. Rev. Lett. **83**, 1159 (1999).

[19] L. J. Onsager, J. A. Chem. Soc. **58**, 1486 (1936).

[20] K. O'Grady, A. Bradbury, S. W. Charles, S. Menear, J. Popplewell, and R. W. Chantrell, J. Magn. Magn. Mater. **31-34**, 958 (1983).

[21] M. S. Wertheim, J. Chem. Phys. **55**, 4291 (1971).

[22] Yu. A. Buyevich and A. O. Ivanov, Physica A **190**, 276 (1992).

[23] A. F. Pshenichnikov, J. Magn. Magn. Mater. **145**, 319 (1995).

[24] K. I. Morozov and A. V. Lebedev, J. Magn. Magn. Mater. **85**, 51 (1990).

[25] M. I. Shliomis, A. F. Pshenichnikov, K. I. Morozov, and I. Y. Shurubor, J. Magn. Magn. Mater. **85**, 40 (1990).

[26] A. F. Pshenichnikov, V. V. Mekhonoshin, and A. V. Lebedev, J. Magn. Magn. Mater. **161**, 94 (1996).

[27] J.-P. Hansen and I. R. McDonald, *Theory of simple liquids*, (Academic Press, 1990), 2nd edition, chapter 4.

[28] S. Banerjee, R. B. Griffiths, and M. Widom, Journ. Stat. Phys. **93**, 109 (1998).

[29] M. Widom and H. Zhang, Phys. Rev. Lett. **74**, 2616 (1995).

[30] B. Groh and S. Dietrich, Phys. Rev. Lett. **74**, 2617 (1995).

[31] H. Zhang and M. Widom, J. Magn. Magn. Mater. **122**, 119 (1993).

[32] H. Zhang and M. Widom, Phys. Rev. E **49**, R3591 (1994).

[33] N. W. Ashcroft and N. D. Mermin, *Solid State Physics*, (Holt, New York, 1976).

[34] V. I. Kalikmanov, Physica A **183**, 25 (1992).

[35] W. H. Keesom, Commun. Phys. Lab. Univ. Leiden, Suppl. **24b**, Section 6 (1915).

[36] J. A. Barker and D. Henderson, Rev. Mod. Phys. **48**, 587 (1976).

FIGURES

FIG. 1. Geometry of our model. Every particle (black) feels the magnetic near field generated by the dipoles of the neighbours (dark gray) within the radius R_s and a contribution from the continuum (light gray) that models the fields of the far–away particles and the external field.

FIG. 2. The first four graphs needed for the expansion of Z in section IV. They correspond to the terms $f_{ij}^{(n)}$ $(n = 0, 1, 2, 3)$, and are of the order $\phi\epsilon^n$.

FIG. 3. The twelve additional graphs needed for an $O(\phi^2, \epsilon^2)$ expansion of Z. The integrals for the crossed out graphs vanish. Graph F vanishes also; see Appendix B6.

FIG. 4. The functions $L_{1,1}$ and $L_{1,2}$ versus α. Note the different scaling.

FIG. 5. The functions $L_{1,n}$ versus α.

FIG. 6. Initial magnetic susceptibility for $\phi = 0.15$ as a function of ϵ.

FIG. 7. The weight of the $O(\phi^2)$–terms that appear in (5.5) are shown versus α. The terms $L_{2,2}^{sphere}$ (5.6b) and $L_{2,2}^{iterative}$ (5.6c) that add up to $L_{2,2}$ (5.6a) are discussed in the text. For comparison, the $O(\phi\epsilon)$–term $L_{1,1}$ is plotted as well.

FIG. 8. The reduced magnetization for $\epsilon = 2$ and $\phi = 0.05$ for moderate α. Taking into account $\phi\epsilon^n$–terms results in a higher magnetization than given by the Langevin function. However, all contributions from the terms $\phi\epsilon^n$ with $n \geq 2$ are almost exactly canceled by the contribution from the second order term $\phi^2\epsilon^2$ for the parameters ϵ, ϕ considered here.

FIG. 9. The reduced susceptibility for $\epsilon = 2$ and $\phi = 0.05$ as a function of α. The higher order corrections are largest at $\alpha = 0$. At moderate α, the cancellation of the terms of order $\phi\epsilon^n$ with $n \geq 2$ against the term of order $\phi^2\epsilon^2$ can again be seen.

FIG. 10. Quality of the lowest order expression (6.5) for the magnetization. (a) shows the isolines of the maximal – with respect to α – ratio (6.6) in steps of 0.01 and (b) shows those of the ratio (6.7).

FIG. 11. Comparison of the effects of polydispersity and of dipolar interaction. Plotted is the reduced magnetization versus α for different ferrofluid models: a noninteracting monodisperse system (only $L_{0,0}$), a noninteracting polydisperse system, and a monodisperse system with dipolar interaction for $\phi = 0.05$ and $\epsilon = 2$. The polydisperse system has a lognormal distribution of particle diameters (eq. 6.8) with a typical width of $\sigma = 0.3$ and the same third moment $\overline{D^3}$ as the monodisperse fluid.

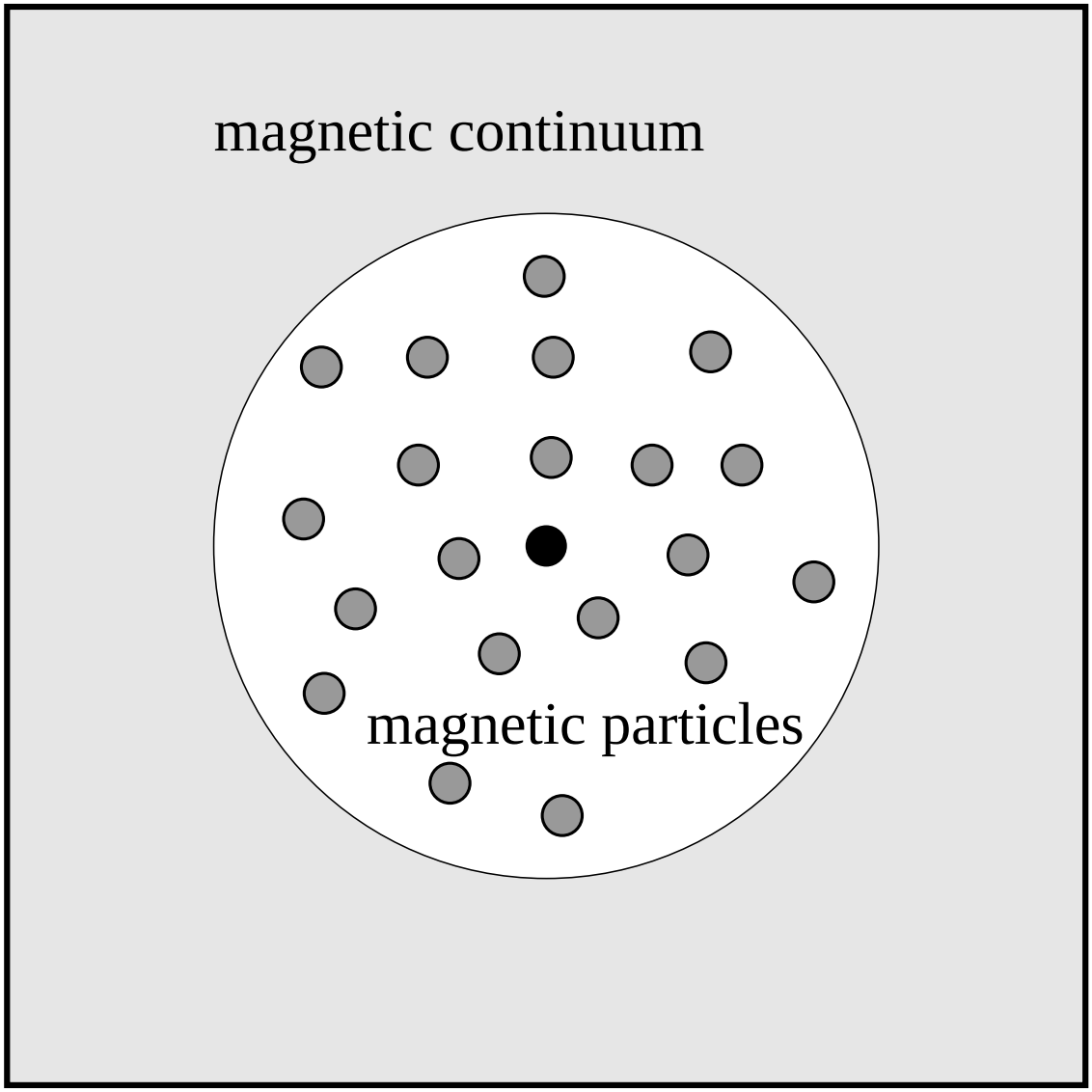

Figure 1
Magnetization of ferrofluids with dipolar interactions ...
B. Huke and M. Lücke, Phys. Rev. E

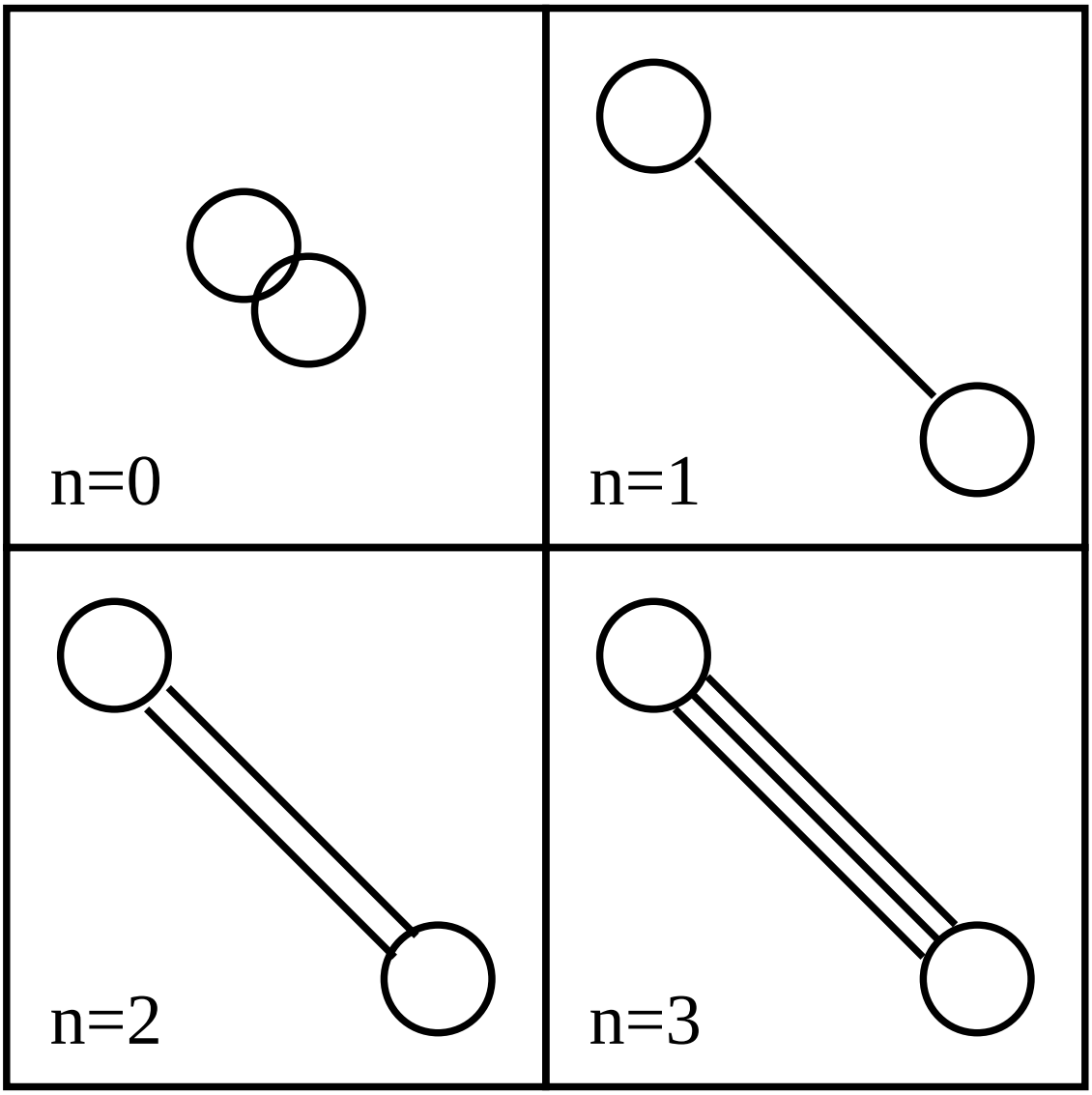

Figure 2
Magnetization of ferrofluids with dipolar interactions ...
B. Huke and M. Lücke, Phys. Rev. E

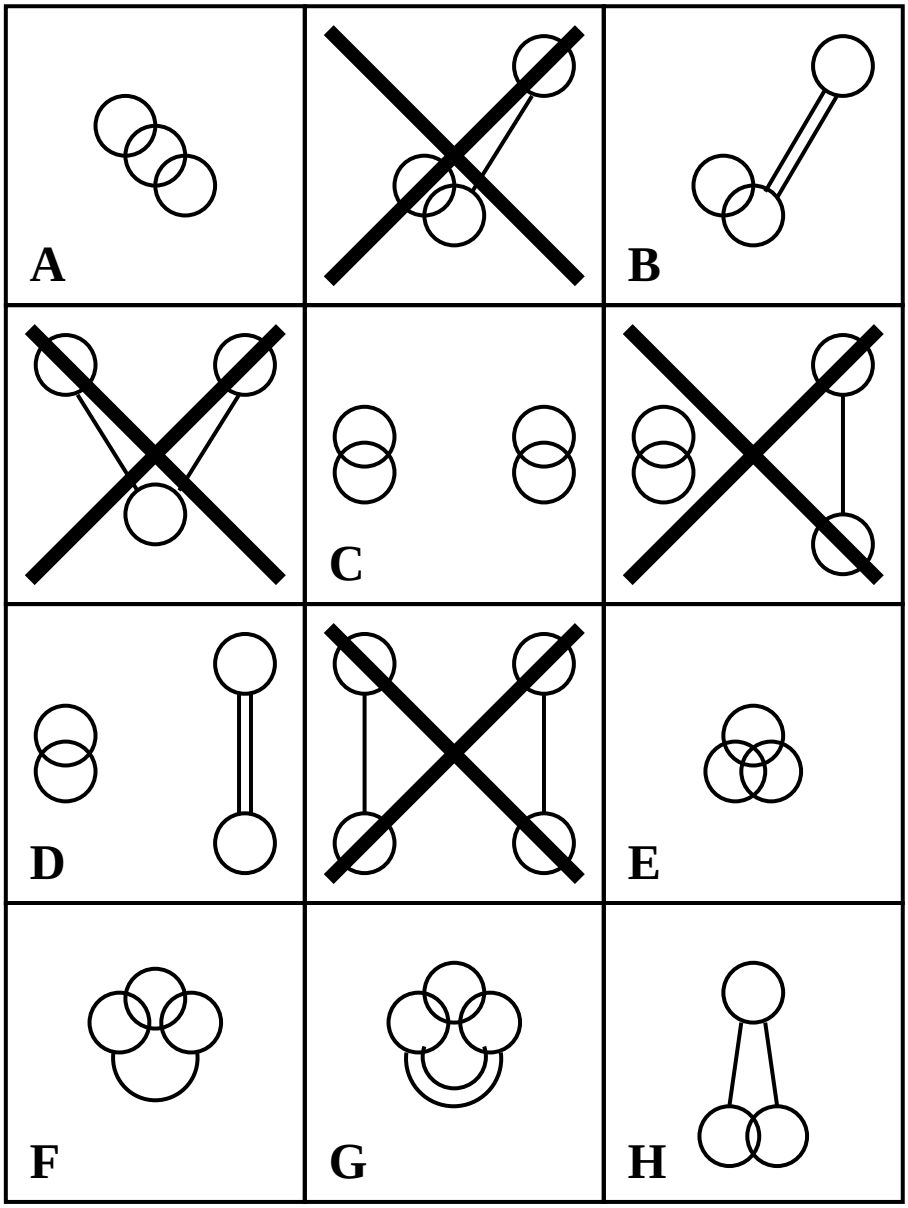

Figure 3
Magnetization of ferrofluids with dipolar interactions ...
B. Huke and M. Lücke, Phys. Rev. E

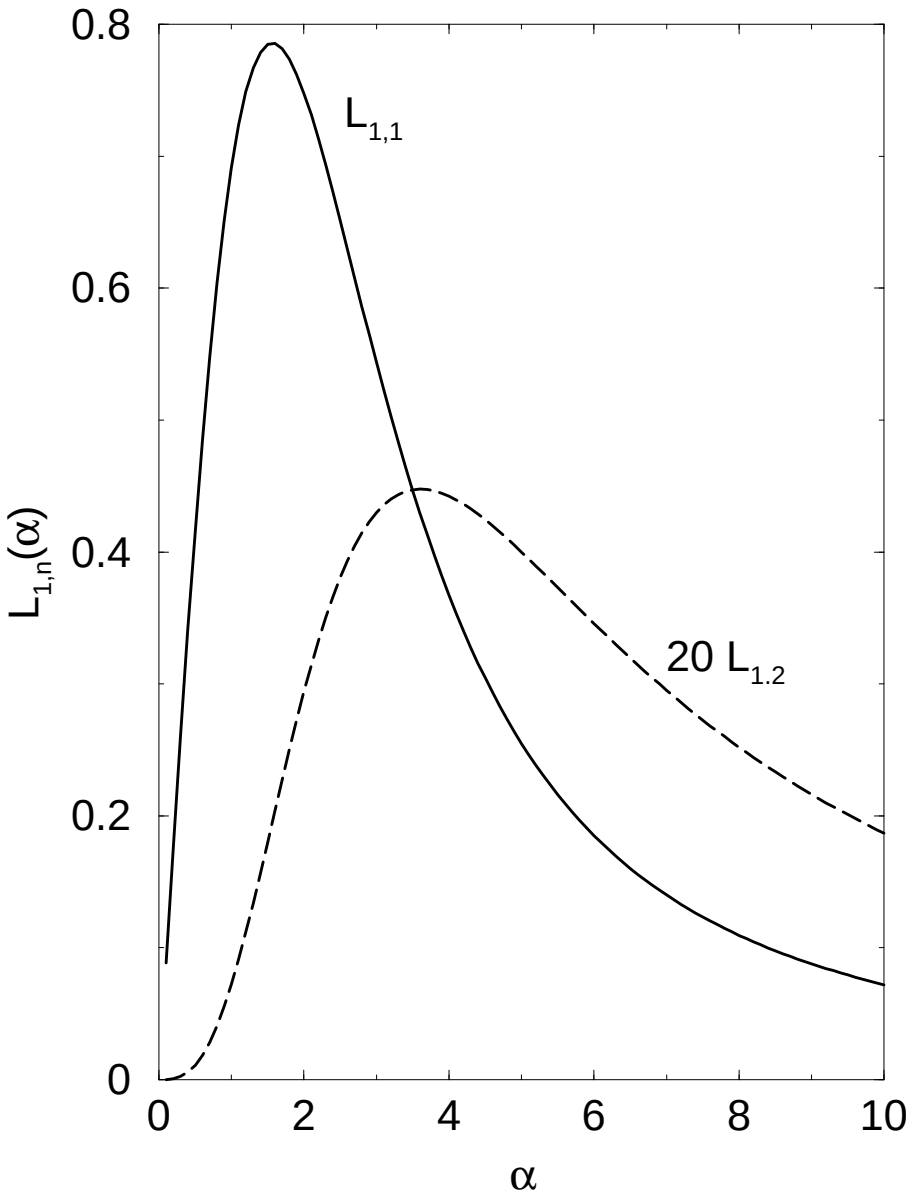

Figure 4
Magnetization of ferrofluids with dipolar interactions ...
B. Huke and M. Lücke, Phys. Rev. E

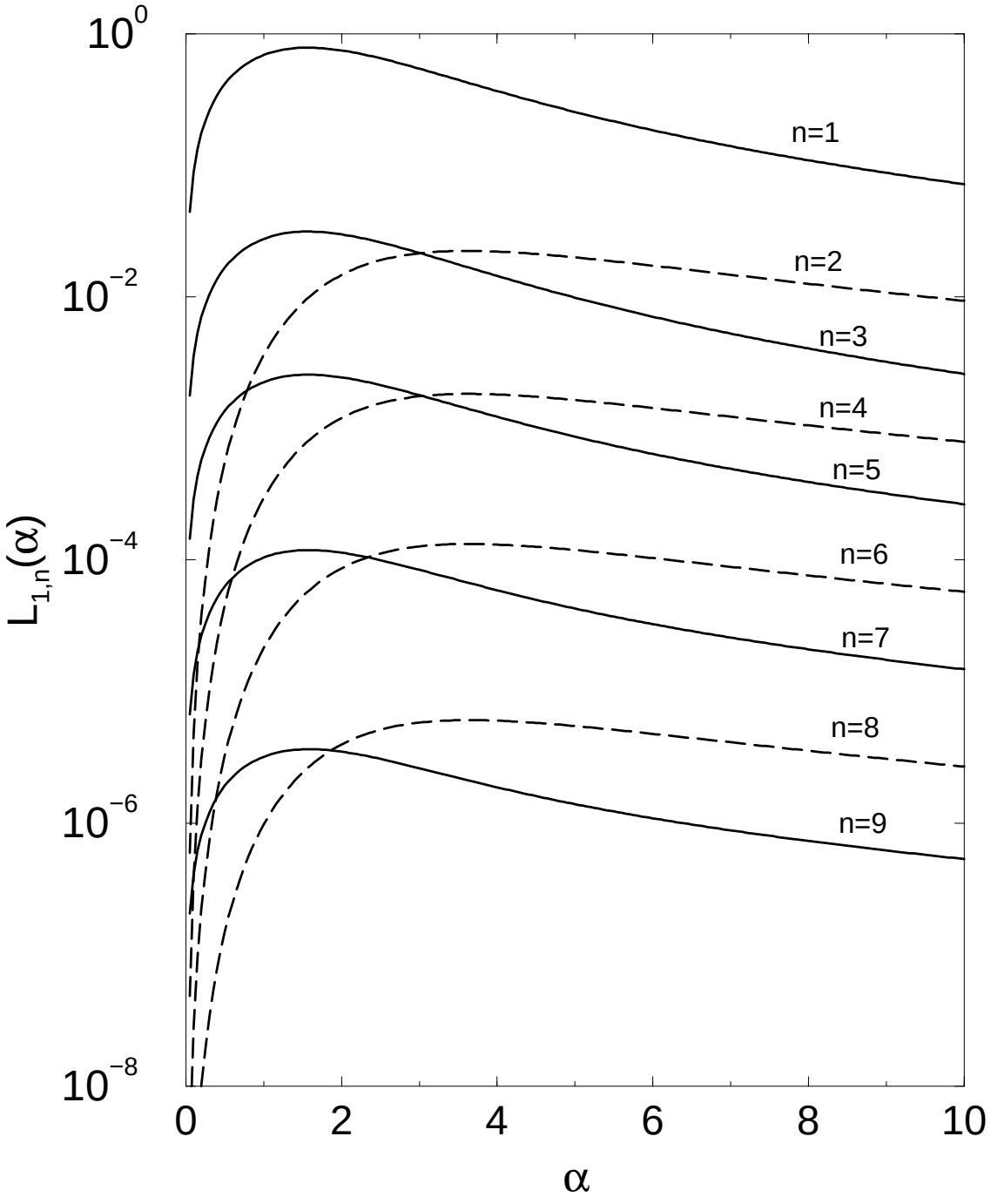

Figure 5
Magnetization of ferrofluids with dipolar interactions ...
B. Huke and M. Lücke, Phys. Rev. E

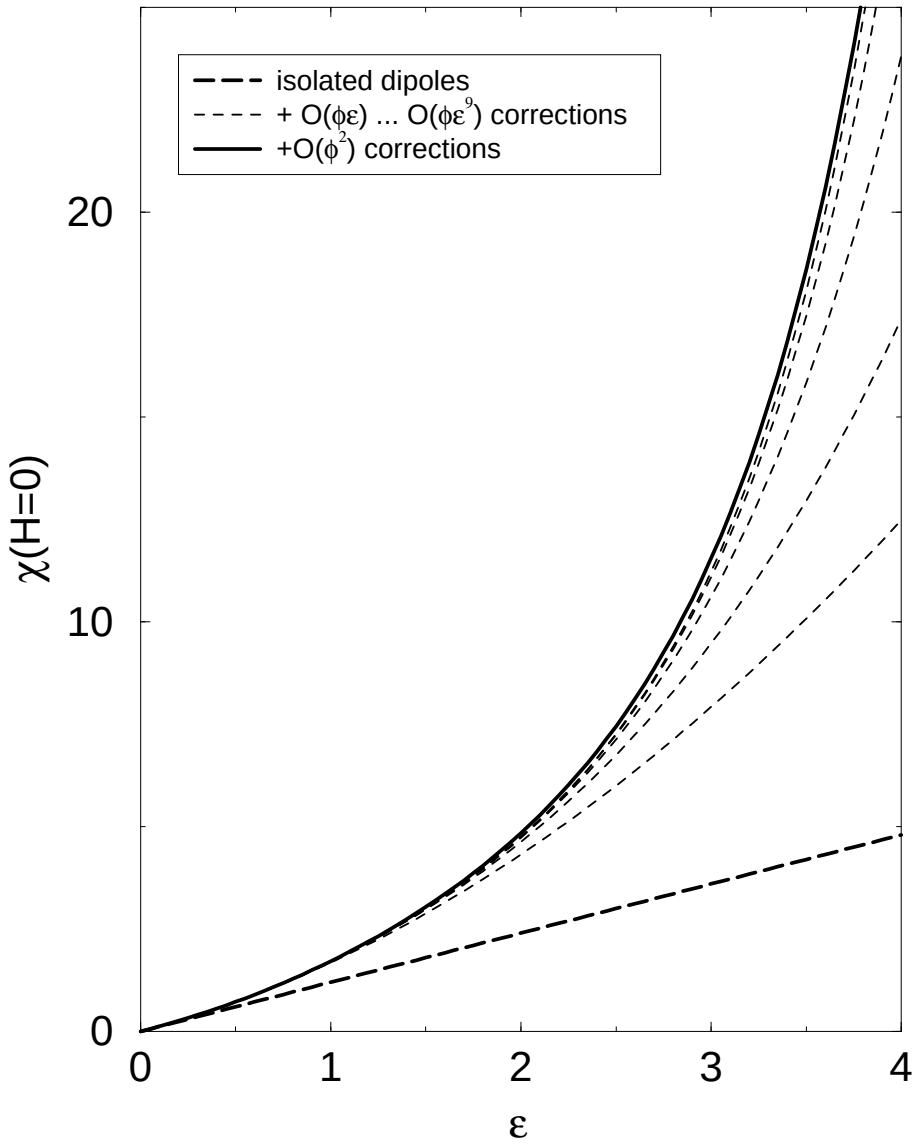

Figure 6
Magnetization of ferrofluids with dipolar interactions ...
B. Huke and M. Lücke, Phys. Rev. E

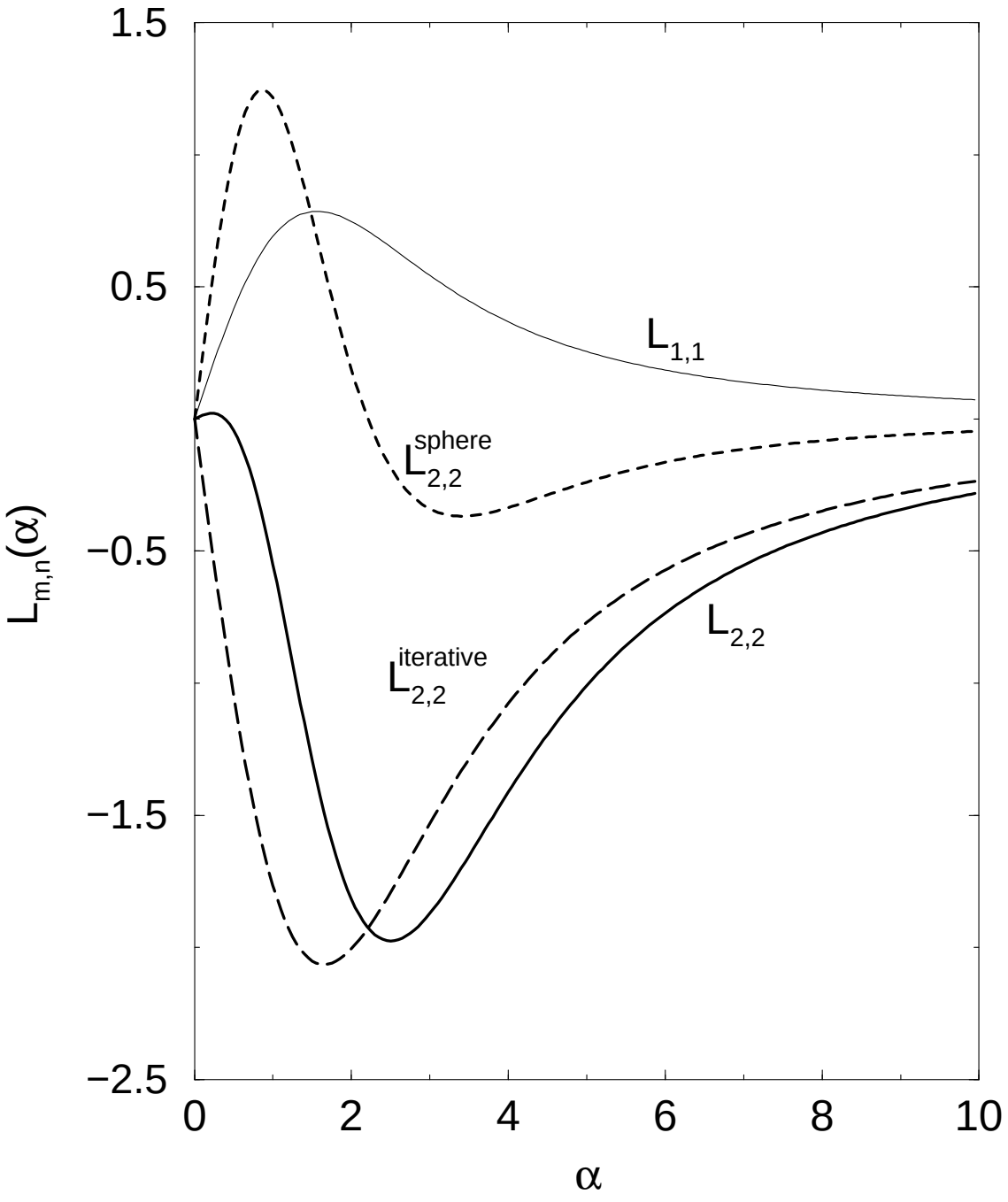

Figure 7
Magnetization of ferrofluids with dipolar interactions ...
B. Huke and M. Lücke, Phys. Rev. E

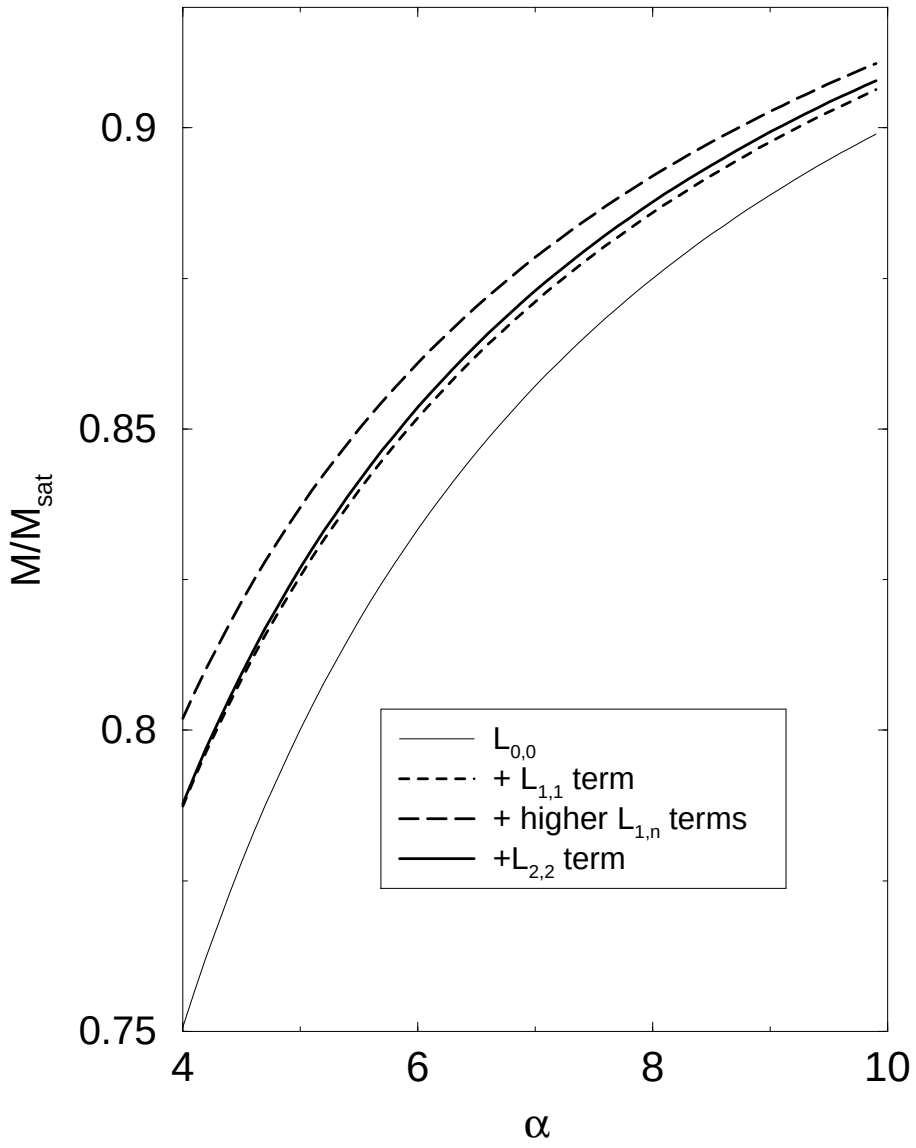

Figure 8
Magnetization of ferrofluids with dipolar interactions ...
B. Huke and M. Lücke, Phys. Rev. E

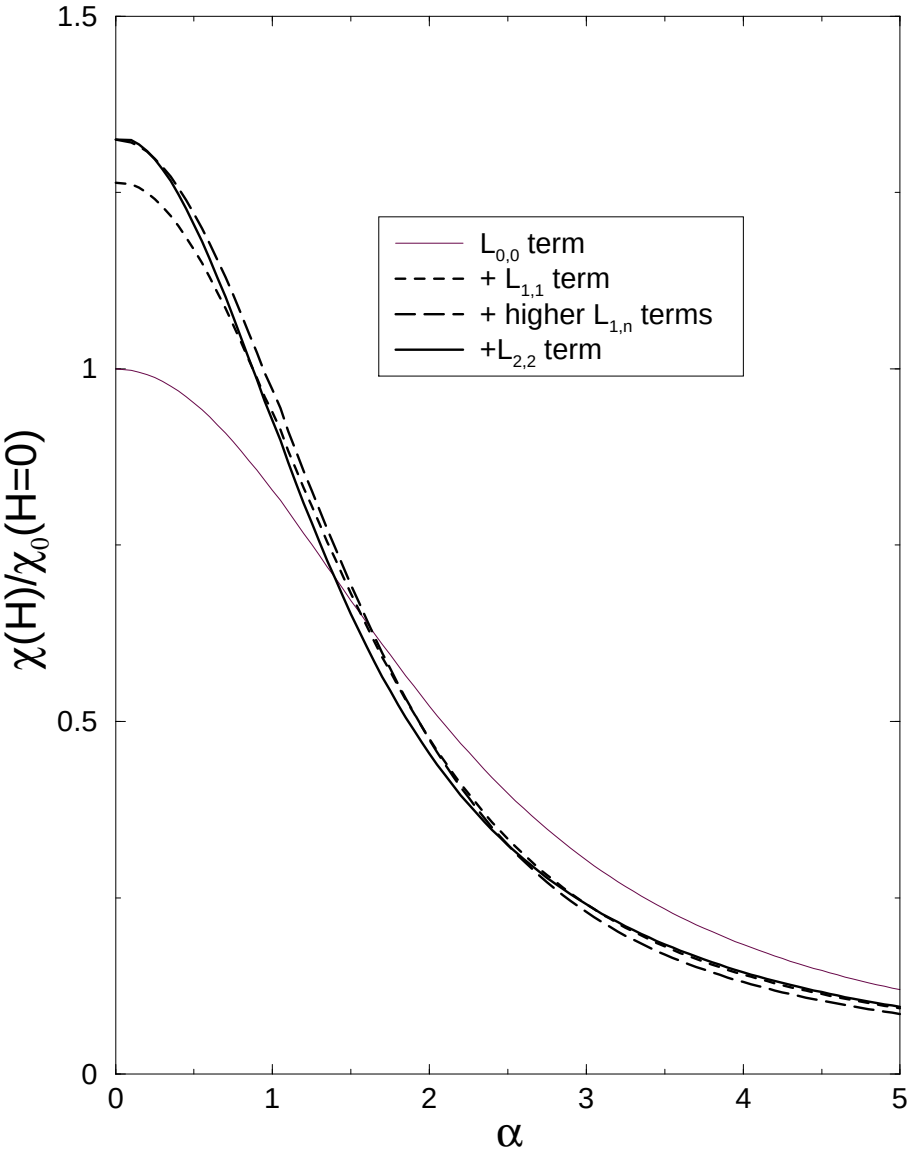

Figure 9
Magnetization of ferrofluids with dipolar interactions ...
B. Huke and M. Lücke, Phys. Rev. E

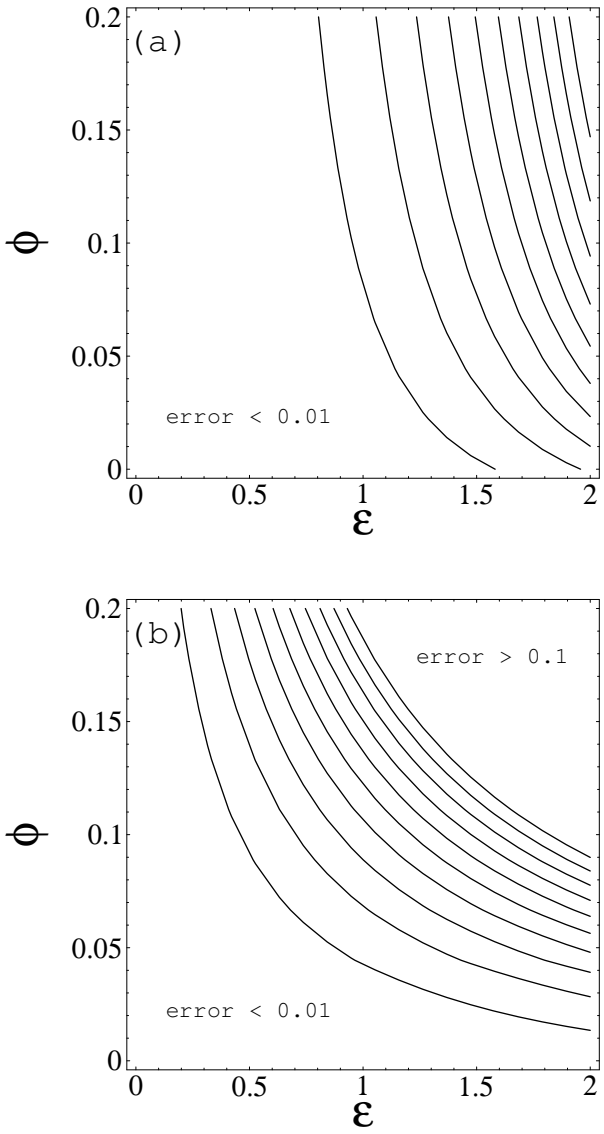

Figure 10
Magnetization of ferrofluids with dipolar interactions ...
B. Huke and M. Lücke, Phys. Rev. E

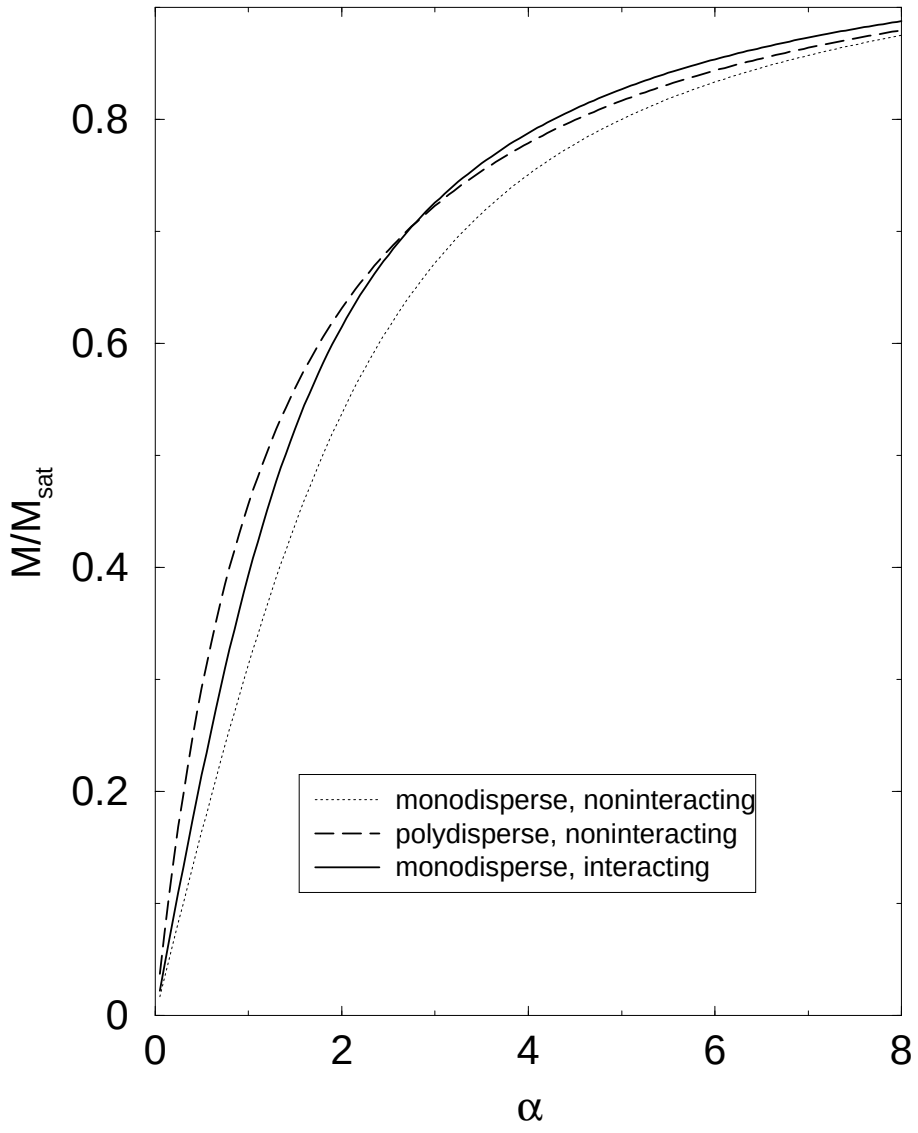

Figure 11
Magnetization of ferrofluids with dipolar interactions ...
B. Huke and M. Lücke, Phys. Rev. E